Journal of Physiology

A cold- and menthol-activated current in rat dorsal root ganglion neurones: properties and role in cold transduction

Gordon Reid, Alexandru Babes and Florentina Pluteanu

Department of Animal Physiology and Biophysics, Faculty of Biology, University of Bucharest, Splaiul Independenţei 91-95, 76201 Bucharest, Romania

Skin temperature is sensed by peripheral thermoreceptors. Using the neuronal soma in primary culture as a model of the receptor terminal, we have investigated the mechanisms of cold transduction in thermoreceptive neurones from rat dorsal root ganglia. Cold-sensitive neurones were pre-selected by screening for an increase in $[Ca^{2+}]_i$ on cooling; 49 % of them were also excited by 0.5 μM capsaicin. Action potentials and voltage-gated currents of cold-sensitive neurones were clearly distinct from those of cold-insensitive neurones. All cold-sensitive neurones expressed an inward current activated by cold and sensitised by (−)-menthol, which was absent from cold-insensitive neurones. This current was carried mainly by Na^+ ions and caused a depolarisation on cooling accompanied by action potentials, inducing voltage-gated Ca^{2+} entry; a minor fraction of Ca^{2+} entry was voltage-independent. Application of (−)-menthol shifted the threshold temperatures of the cold-induced depolarisation and the inward current to the same extent, indicating that the cold- and menthol-activated current normally sets the threshold temperature for depolarisation during cooling. The action of menthol was stereospecific, with the (+)-isomer being a less effective agonist than the (−)-isomer. Extracellular Ca^{2+} modulated the cold- and menthol-activated current in a similar way to its action on intact cold receptors: lowered $[Ca^{2+}]_o$ sensitised the current, while raised $[Ca^{2+}]_o$ antagonised the menthol-induced sensitisation. During long cooling pulses the current showed adaptation, which depended on extracellular Ca^{2+} and was mediated by a rise in $[Ca^{2+}]_i$. This adaptation consisted of a shift in the temperature sensitivity of the channel. In capsaicin-sensitive neurones, capsaicin application caused a profound depression of the cold-activated current. Inclusion of nerve growth factor in the culture medium shifted the threshold of the cold-activated current towards warmer temperatures. The current was blocked by 50 μM capsazepine and 100 μM SKF 96365. We conclude that the cold- and menthol-activated current is the major mechanism responsible for cold-induced depolarisation in DRG neurones, and largely accounts for the known transduction properties of intact cold receptors.

Cooling of the skin is detected by cutaneous cold receptors, which include both Aδ- and C-fibres (Hensel & Zotterman, 1951*b*; Iriuchijima & Zotterman, 1960). The responses of these receptors to thermal stimuli have been intensively studied (reviewed by Hensel, 1981; Darian-Smith, 1984) and attempts have been made to deduce their transduction mechanisms from action potential activity in response to cold and menthol, a cold receptor stimulant (Braun *et al.* 1980; Schäfer *et al.* 1984; Schäfer *et al.* 1986). However, the difficulty of recording at the membrane level from cold receptor terminals has hampered progress until recently. Rapid progress is now being made with the help of a convenient and widely used model, the soma of a primary sensory neurone (from dorsal root ganglion, DRG, or trigeminal ganglion, TG) kept in short-term culture. The cultured soma takes on the properties of its former peripheral receptor, apparently by expressing in its

membrane proteins that would normally have been transported to the receptor terminal (Baccaglini & Hogan, 1983; Cesare & McNaughton, 1997).

Cold transduction in this model involves at least three mechanisms. Firstly, a cold-activated non-selective cation channel is expressed in cold-sensitive DRG neurones (Reid & Flonta, 2001*a*; Okazawa *et al.* 2002; Reid & Flonta, 2002). This channel is sensitised by menthol (Reid & Flonta, 2001*a*; Reid & Flonta, 2002); a cold- and menthol-activated current has also been described in TG neurones (McKemy *et al.* 2002). The ion channel that probably underlies the native current, a member of the TRP (transient receptor potential) family, has recently been cloned from TG and DRG (McKemy *et al.* 2002; Peier *et al.* 2002) and named CMR-1 (cold and menthol receptor 1) or TRPM8 (according to the unified nomenclature for

TRP channels). Cold and menthol activate the native channel directly or via a membrane-delimited mechanism, but modulation by the cellular environment is important for normal temperature sensitivity and adaptation (Reid & Flonta, 2002).

A second mechanism is the inhibition by cold of a temperature-sensitive background K$^+$ conductance; this has been described in both DRG (Reid & Flonta, 2001*b*) and TG (Viana *et al.* 2002), and supports an earlier suggestion that TREK-1, a background K$^+$ channel strongly inhibited by cooling, may be involved in cold sensing (Maingret *et al.* 2000). Thirdly, inhibition of the Na$^+$–K$^+$-ATPase alters the activity of cold receptors in amphibians and mammals, suggesting that its inhibition by cold may have a role in cold transduction (Pierau *et al.* 1974; Spray, 1974; Pierau *et al.* 1975; Schäfer & Braun, 1990); Na$^+$–K$^+$-ATPase inhibition also depolarises cold-sensitive DRG neurones, although its role in this model appears to be a minor one (Reid & Flonta, 2001*b*).

Differential expression of voltage-gated ion channels is likely to influence cold receptor behaviour: lower expression of voltage-gated K$^+$ channels makes cold-sensitive TG neurones more excitable than cold-insensitive neurones of similar size, and the hyperpolarisation-activated cation current I_h is larger in cold-sensitive than cold-insensitive TG neurones (Viana *et al.* 2002). How these factors interact with specific transduction mechanisms to determine cold receptor sensitivity and specificity is not yet well understood.

In the present study we have investigated the properties of cold-sensitive neurones in DRG cultures, in particular the native cold- and menthol-activated current and the ion channels that underlie it, and the role of this current in cold transduction.

METHODS

DRG culture

Adult male Wistar rats (150–250 g) were killed by inhalation of 100 % CO_2 followed by decapitation and exsanguination, following UK Home Office approved (Schedule 1) procedure in the absence of any national or institutional animal welfare guidelines. DRGs from spinal levels L1–S1, inclusive, were removed (Lindsay *et al.* 1991) and incubated in 0.6 mg ml^{-1} collagenase (Sigma type XI) and 3 mg ml^{-1} Dispase (non-specific protease) for 1 h at 37 °C in standard extracellular solution (see below). After trituration the dissociated cells were plated onto borosilicate glass coverslips (0.17 mm thick) which had been treated with poly-D-lysine (0.1 mg ml^{-1} for 30 min), and cultured (37 °C, 5 % CO_2 in air) in a 1:1 mixture of Dulbecco's modified Eagle's medium and Ham's F12 medium with 10 % horse serum and 50 μg ml^{-1} gentamicin. Unless stated otherwise in Results, 50 ng ml^{-1} nerve growth factor (NGF) 7S was added to the medium just before the cells were plated, from a frozen 10 μg ml^{-1} stock solution in serum-containing culture medium. All items for the cultures were obtained from Sigma. Recordings were made after 2–4 days in culture.

Intracellular Ca^{2+} imaging and pre-selection of cold-sensitive neurones

Coverslips with attached cells were incubated for 30 min at 37 °C in standard extracellular solution (see below) containing 2 μM Calcium Green-1 AM and 0.02 % Pluronic (both from Molecular Probes, Leiden, the Netherlands). After dye loading, they were left in the incubator for at least 30 min before use. Coverslips were then mounted in a Teflon chamber (MSC–TD, Digitimer, Welwyn Garden City, UK) on the stage of a Nikon TE 200 inverted microscope and adapted for ⩾ 5 min at a base temperature of 32 °C, close to normal mammalian skin temperature, before applying cooling stimuli. Temperature was controlled by local superfusion with a Peltier-based system that has already been described (Reid *et al.* 2001); solutions were applied at 0.8–1 ml min^{-1} through a 1 mm i.d. tube placed 1 mm from the neurone, and the suction system to maintain constant fluid level during superfusion was based on that described by Ruppersberg & Rudel (1983). To avoid adding electrical noise by placing a thermocouple in the bath during recordings, we measured stimulus temperature after the experiment by repeating all thermal stimuli with a miniature T-type thermocouple (IT-1E, 50 μm wire diameter, accurate to 0.1 °C; Physitemp, Clifton, NJ, USA) placed where the cell had been. This method also gives a more accurate estimate of cell temperature during the recording than would be obtained by placing a thermocouple near the cell and recording the temperature simultaneously: reproducibility of successive thermal stimuli is very good, whereas marked spatial and temporal variations of temperature exist between the application system and the bath (Reid *et al.* 2001). Unless stated otherwise, the thermal stimulus was a cooling ramp to ~18 °C at ~0.5 °C s^{-1}, preceded by a brief (~10 s) warming to 37–38 °C; the warming step was introduced to inhibit the menthol-induced current and allow its threshold temperature to be measured, and was used in all further measurements to ensure consistency.

Neurones were illuminated using the standard mercury vapour lamp of the microscope and a standard fluorescein filter set (Nikon B2A), and viewed with a dry objective (× 40, NA 0.95). Images were collected using a COHU 4910 camera (COHU, San Diego, CA, USA) and MuTech 450 Pro frame grabber (MuTech Corp. Billerica, MA, USA), using software written by G. R. and analysed using programs written in the IDL language (version 5.3, Research Systems, Boulder, CO, USA). In later experiments the light source was replaced by a 100 W halogen lamp and filter wheel (Cairn Research, Faversham, UK) controlled by Axon Imaging Workbench software (version 2.2, Axon Instruments, Union City, CA, USA) which was also used for image acquisition and analysis.

Before recording fluorescent images from a field of cells, a phase-contrast image of the field was recorded with the same objective to allow cell diameters to be measured. Mean diameter was estimated from cell area (which was measured using a program written in IDL and assumed to be equal to πr^2); for this reason, diameters of neurones located on the edge of a field of view could sometimes not be measured.

Patch clamp recording

Patch clamp recordings were made using borosilicate glass pipettes (GC150T, Harvard Apparatus) polished to a resistance of 2–4 MΩ; for recordings in membrane patches, pipettes were coated with Sylgard 184 (World Precision Instruments, Berlin, Germany). Currents were recorded with an EPC-7 amplifier (HEKA, Lambrecht, Germany) or a PCA-100 amplifier (ESF electronic, Göttingen, Germany). After filtering the current at

3 kHz (3-pole Bessel filter) we digitized the signals with a Labmaster 160 kHz DMA interface (Scientific Solutions, Mentor, OH, USA) using software written by G. R. which was also used to control the thermal stimulator. When recording from membrane patches, we filtered the current signal at 10 kHz (3-pole Bessel) and recorded current and temperature on a modified Sony PCM 701ES audio processor and standard video recorder. This tape recording was later re-sampled off-line at 40 kHz with GATHER software (Scientific Solutions). Analysis was carried out with programs written in IDL or with Clampfit (version 6.0, Axon Instruments).

Unless stated otherwise in Results, all whole-cell recordings were made with the amphotericin perforated patch configuration (Rae *et al.* 1991), back-filling the pipette with amphotericin B-containing solution (240 μg ml^{-1} amphotericin (Sigma) with 0.02 % Pluronic) after first filling the tip with amphotericin-free solution. Final access resistances were in the range 10–15 MΩ, giving series resistance errors for peak cold-induced currents of around 1–5 mV; series resistance was not compensated. Pluronic was used because it greatly improved the speed and reliability of amphotericin permeabilisation. In separate control experiments ($n = 5$), we verified that Pluronic without amphotericin did not permeabilise the membrane over a period of 30 min.

We used the conventional whole-cell configuration in two series of experiments: firstly, to record voltage-dependent currents, which were often large and fast, where minimizing series resistance was important; secondly, the whole-cell configuration was used in experiments on adaptation involving BAPTA- and EGTA-containing pipette solutions, where exchange of solution between pipette and cell was necessary. A few measurements using candidate blockers or Na$^+$-free solutions were made after recording voltage-gated currents, and these are noted as they occur in Results.

Solutions

Standard extracellular solution contained (mM): NaCl 140, KCl 4, CaCl$_2$ 2, MgCl$_2$ 1, Hepes 10, NaOH 4.55. This was used in all recordings unless stated otherwise. Sodium-free solutions were prepared by replacing all the Na$^+$ by (a) choline, (b) *N*-methyl-D-glucamine (NMDG) or (c) tetramethylammonium (TMA). Their composition was (mM): (a) choline chloride 140, KOH 4, NMDG 0.5, CaCl$_2$ 2, MgCl$_2$ 1, Hepes 10; (b) NMDG 140, HCl 135, KCl 4, CaCl$_2$ 2, MgCl$_2$ 1, Hepes 10 and (c) TMA-OH 140, HCl 140, KCl 4, CaCl$_2$ 2, MgCl$_2$ 1, Hepes 10. The pH of all external solutions was 7.4 at 25 °C. The pipette solution for amphotericin perforated-patch recording contained (mM): K$_2$SO$_4$ 60, KCl 35, NaCl 10, MgCl$_2$ 1, sucrose 20, Hepes 10, EGTA 1, NaOH 3.45, KOH 2.35 (pH 7.2 at 25 °C); the same solution was used in conventional whole-cell mode to record voltage-gated currents and action potentials. The pipette solution for outside-out patches contained (mM): CsCl 140, NaCl 6, Hepes 10, EGTA 2, NaOH 7.6, pH 7.2 at 25 °C. A solution based on this was used for the adaptation experiments with 10 mM BAPTA or EGTA (mM): NaCl 13, Hepes 10, EGTA or BAPTA 10, CsOH 24 (EGTA) or 43 (BAPTA), CsCl 116 (EGTA) or 97 (BAPTA); total [Cs$^+$] was 140 mM in each case, pH 7.2 at 25 °C. Pipette solutions did not contain ATP or GTP.

Drugs were added from the following stock solutions: (−)-menthol (Sigma), (+)-menthol (TCI, Tokyo, Japan) or cyclohexanol (Fluka), 200 mM in ethanol; capsaicin (Sigma), 10 mM in ethanol; capsazepine (Sigma), 100 mM in DMSO; SKF 96365 (Tocris, Bristol, UK), 10 mM in standard extracellular solution. All drug

dilutions were prepared on the day of the experiment and menthol- and cyclohexanol-containing solutions were renewed every 2 h because of evaporation.

Statistics

All measurements are given as means ± S.D.; statistical significance was tested using Student's *t* test (paired or unpaired as appropriate) or the χ^2 test, and correlations were calculated using Spearman's rank correlation coefficient. A value of $P < 0.05$ was considered to be statistically significant.

RESULTS

Pre-selection of cold-sensitive and cold-insensitive DRG neurones by [Ca^{2+}]$_i$ imaging

The change in Calcium Green fluorescence on cooling (ΔF) was measured as a fraction of that just before the stimulus (F_0; Takahashi *et al.* 1999). Even at constant [Ca^{2+}]$_i$, a change in fluorescence intensity is expected on cooling due to the opposing effects of temperature on the effective dissociation constant for Ca^{2+} (Harrison & Bers, 1987; Lattanzio, 1990; Shuttleworth & Thompson, 1991) and on the lifetime of the excited state of the dye (Oliver *et al.* 2000). We therefore selected neurones based on whether they showed a clear non-linear increase in $\Delta F/F_0$ during cooling at a distinct threshold temperature (see Fig. 1*D* and *E*). From a consecutive series of recordings in which $\Delta F/F_0$ was measured in every one of 923 neurones, we found 70 showing this 'threshold' behaviour (peak $\Delta F/F_0 = 0.40 \pm 0.17$, mean ± S.D.) while the remainder showed a small increase or decrease in $\Delta F/F_0$ on cooling with a near-linear relation to the thermal stimulus (peak $\Delta F/F_0 = 0.013 \pm 0.068$, $n = 853$), which can be accounted for by the physical processes mentioned above. Both groups were normally distributed. Neurones in the 'threshold' group were considered as possibly cold-sensitive, and those in the 'no threshold' group as probably insensitive to cooling.

To define two distinct groups as cold-sensitive and cold-insensitive, we derived a cutoff value of $\Delta F/F_0$ from the mean plus two standard deviations of the 'no threshold' group ($\Delta F/F_0 = 0.013 + 2 \times 0.068 = 0.149$). We therefore defined neurones with a non-linear increase in $\Delta F/F_0$ starting at a distinct threshold temperature, and peak $\Delta F/F_0 \geqslant 0.15$, as cold-sensitive (67/923, 7.3 %); those with no distinct threshold and $\Delta F/F_0 < 0.15$ were defined as cold-insensitive (826/923, 89.5 %). The remaining neurones (30/923, 3.3 %) were considered to be of uncertain status and not studied further.

As detailed in Supplementary Information:

http://www.jphysiol.org/cgi/content/full/545/2/595

$\Delta F/F_0$ was measured in a total of 2664 neurones for this study, 421 in the 'threshold' group and 2243 in the 'no threshold' group; 386 were classified by the criteria above as cold-sensitive and 2157 as cold-insensitive, with the remaining 121 neurones remaining unclassified (see Fig. 1*E*).

Table 1. Characteristics of neurones sensitive and insensitive to cold, 100 μM (–)-menthol and 0.5 μM capsaicin

	Cold-sensitive	n	Cold-insensitive	n	$P*$
Diameter (all neurones) (μm)	19.7 ± 3.9	331	24.7 ± 6.7	1106	< 0.001
Diameter (neurones treated with menthol and/or capsaicin) (μm)	21.4 ± 5.6	39	25.9 ± 6.7	241	< 0.001
Diameter (capsaicin-sensitive only) (μm)	20.5 ± 4.9	18	24.6 ± 5.8	119	0.005
Diameter (capsaicin-insensitive only) (μm)	21.5 ± 5.4 **	20	—	—	—
Number of menthol-sensitive neurones	27/38 (71 %)	—	5/254 (2 %)	—	< 0.001 (χ^2 test)
Number of capsaicin-sensitive neurones	19/39 (49 %)	—	123/236 (52 %)	—	n.s. (χ^2 test)
$\Delta F/F_0$ capsaicin	0.219 ± 0.331	39	0.278 ± 0.332	236	n.s.
	Menthol-sensitive		Menthol-insensitive		
Cold threshold (cold-sensitive only) (ºC)	30.4 ± 2.1	27	25.6 ± 2.9	11	< 0.001
	Capsaicin-sensitive		Capsaicin-insensitive		
Cold threshold (cold-sensitive only) (ºC)	27.8 ± 3.1	19	30.6 ± 2.7	20	< 0.001

* Student's unpaired t test unless stated. **$P = 0.56$ *vs.* cold- and capsaicin-sensitive neurones.

Each section below describes measurements made in a subset of these 386 cold-sensitive or 2157 cold-insensitive neurones, except the section on 'Action potentials and voltage-gated currents' which was based on a separate group of 108 neurones not pre-selected by $[Ca^{2+}]_i$ imaging.

Most cold-sensitive neurones were dark with a clearly visible nucleus, although other neurones of similar size and with apparently identical morphology were insensitive to cold (Fig. 1*A*). Cold-sensitive neurones were significantly smaller than cold-insensitive neurones (Fig. 1*F* and Table 1).
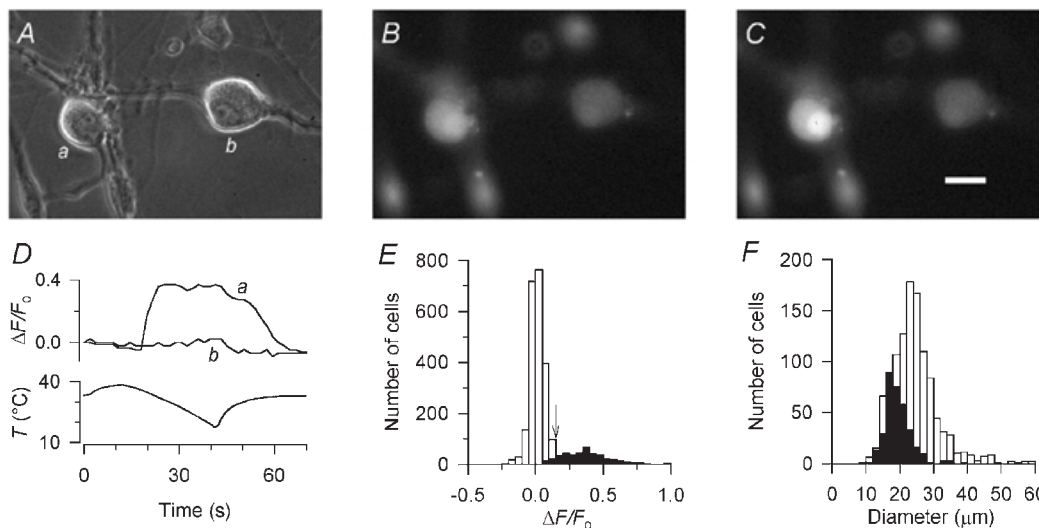
Figure 1. Responses of rat dorsal root ganglion neurones to cooling

A, phase contrast image of two DRG neurones after 2 days in culture. *B*, epifluoresence image of the same two neurones, loaded with Calcium Green-1, just before applying the cooling stimulus. *C*, the same neurones at the peak of the cold stimulus. Scale bar 20 μm. *D*, ratio of the fluorescence change during the cold stimulus (ΔF) to the fluorescence intensity before the stimulus (F_0) for the two neurones shown in *A–C*. Neurone *a* was defined as cold-sensitive according to the criteria described in Results, while neurone *b* was defined as insensitive to cold. In all cases, fluorescence intensity was averaged over the cytoplasmic area of the neurone excluding the nucleus, in order to measure only the change in cytoplasmic $[Ca^{2+}]_i$. *E*, histogram of $\Delta F/F_0$ in 2664 DRG neurones, 421 from the 'threshold' group (■) and 2243 from the 'no-threshold' group (□; see text for definitions). The cutoff point for defining a neurone as cold-sensitive ($\Delta F/F_0 \geqslant 0.15$) is arrowed; neurones in the 'threshold' group with peak $\Delta F/F_0 \geqslant 0.15$ were considered as cold-sensitive (see Results). *F*, histogram of the diameters of 331 cold-sensitive neurones (■) and 1106 cold-insensitive neurones (□); cold-sensitive neurones were among the smallest in DRG cultures.

Table 2. Action potentials and voltage-gated currents in cold-sensitive and cold-insensitive DRG neurones

	Cold-sensitive	*n*	Cold-insensitive	*n*	*P**
Diameter (μm)	18.8 ± 1.6	32	20.7 ± 2.2	60	< 0.001
Action potential parameters:					
Resting potential (mV)	-53.0 ± 7.0	21	-51.6 ± 5.0	38	n.s.
Amplitude (mV)	93.2 ± 13.6	21	89.3 ± 11.6	38	n.s.
Duration at takeoff voltage (ms)	3.6 ± 1.5	21	4.5 ± 1.3	38	0.015
After-hyperpolarisation (AHP) (mV)	4.4 ± 2.9 **	16	12.9 ± 4.7	38	< 0.001
AHP duration (at 80 % return to resting potential) (ms)	100 ± 96 **	13	112 ± 68	38	n.s.
Number showing inflection	8/21 (38 %)		27/38 (71 %)		< 0.001 (χ^2 test)
Voltage-gated currents:					
I_h amplitude (pA)	106 ± 79	33	71.4 ± 47	63	0.008
Decay time constant of transient inward current (ms)	0.9 ± 0.2	32	2.3 ± 0.9	63	< 0.001
Number expressing A-type K$^+$ current	14/33 (42 %)		50/64 (78 %)		< 0.001 (χ^2 test)
Cold-sensitive neurones only:	Capsaicin-sensitive		Capsaicin-insensitive		
I_h amplitude (pA)	90.0 ± 55	14	191 ± 89	7	0.004
Action potential duration (ms)	3.1 ± 0.7	14	4.5 ± 2.2	7	0.04

* Student's unpaired *t* test unless stated; ** AHP absent in 5 neurones and too small to measure duration in a further 3 neurones.

[Ca^{2+}]$_i$ responses to menthol and capsaicin in cold-sensitive neurones

We imaged [Ca^{2+}]$_i$ while applying the cold receptor stimulant ($-$)-menthol and/or capsaicin, the active ingredient from hot chilli peppers, to 298 neurones, of which 40 were cold-sensitive. The agonists were applied at 32 °C and positive responses were defined arbitrarily as $\Delta F/F_0 \geqslant 0.1$. The majority of cold-sensitive neurones (71 %) reacted to menthol at this temperature but very few cold-insensitive neurones (2 %) reacted, while about half of each group responded to capsaicin (Table 1).

Co-expression of cold and menthol sensitivity was highly significant, while cold-sensitive neurones did not differ from cold-insensitive neurones in their responses to capsaicin (Table 1). Among cold-sensitive neurones, the amplitudes of [Ca^{2+}]$_i$ responses to menthol and capsaicin were negatively correlated (Fig. 2*A*), and were also significantly correlated (positively and negatively, respectively) with the threshold temperature of the [Ca^{2+}]$_i$ increase during cooling (Fig. 2*B* and *C*); threshold temperature was measured at the start of the exposure for the first frame where $\Delta F/F_0$ began to deviate from zero by an extent exceeding the frame-to-frame noise. Neurones responding to menthol at 32 °C were significantly more cold-sensitive than those that did not respond, while capsaicin-sensitive neurones required stronger cooling to stimulate them than capsaicin-insensitive neurones (Table 1).

Within the group of capsaicin-responsive neurones, there was a clear size difference between those that were sensitive and insensitive to cold. The diameters of cold-sensitive neurones were significantly smaller than those of cold-insensitive neurones, but indistinguishable from those of cold-sensitive neurones that were insensitive to capsaicin (Table 1).

Action potentials and voltage-gated currents in cold-sensitive and cold-insensitive neurones

The time course of the action potential and the pattern of expression of voltage-gated currents correlate with function among DRG neurones and have been used to identify discrete groups of neurones by their 'current signature' (Cardenas *et al.* 1995; Djouhri *et al.* 1998; Petruska *et al.* 2000*b*). To test whether cold-sensitive neurones belong to one of these previously identified groups of cells, we measured action potentials and voltage-gated currents using conventional whole-cell (not perforated-patch) recording in 108 DRG neurones of around 20 μm diameter (20.0 ± 2.2 μm; $n = 92$), which had not been pre-selected by [Ca^{2+}]$_i$ imaging. We chose this size range because it includes the largest proportion of cold-sensitive neurones (see Fig. 1*F*). We classified as cold-sensitive those firing more than ten action potentials during cooling (33/108, 31 %) while those that did not fire action potentials and were depolarised by less than 5 mV were classified as cold-insensitive (64/108, 59 %). Even within this group of small-diameter cells, cold-sensitive neurones were significantly smaller than cold-insensitive neurones (Table 2).

Action potentials of cold-sensitive neurones, measured at 32 °C, were of significantly shorter duration than those
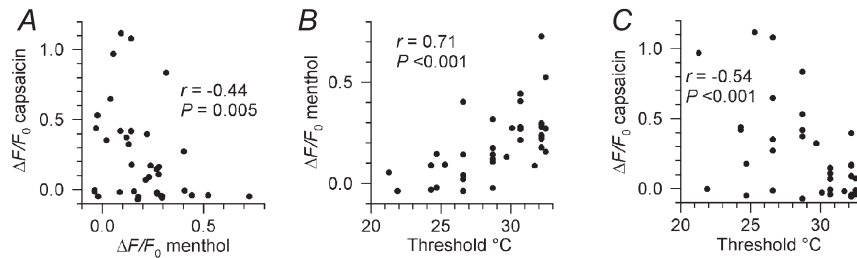
Figure 2. The relationship between cold, menthol and capsaicin sensitivity

A, correlation between the amplitudes of the increases in $[Ca^{2+}]_i$ (expressed as $\Delta F/F_0$) induced by 100 μM (−)-menthol and 0.5 μM capsaicin in cold-sensitive neurones. *B* and *C*, correlations between the rise in $[Ca^{2+}]_i$ induced by menthol (*B*) and capsaicin (*C*) and the threshold temperature at which $[Ca^{2+}]_i$ began to rise during cooling. Spearman rank correlation coefficients (*r*) are shown on each plot, along with the statistical significance (*P*) of the correlations.

of cold-insensitive neurones (measured at the takeoff voltage), and significantly fewer showed an inflection during repolarisation (defined as an abrupt transition from a smaller to a larger negative value of d*V*/d*t* during repolarisation; see Table 2 and Fig. 3*A*). There was no difference between the groups in after-hyperpolarisation (AHP) duration, measured at 80 % return to the resting potential, but the amplitude of the AHP (measured from the resting potential to the peak AHP) was conspicuously smaller in cold-sensitive neurones, and 5 of 21 showed a small depolarising rather than hyperpolarising after-potential.

Voltage-dependent currents were measured with the pulse protocols used by Petruska *et al.* (2000*b*), which are described in the figure legends. The characteristic features
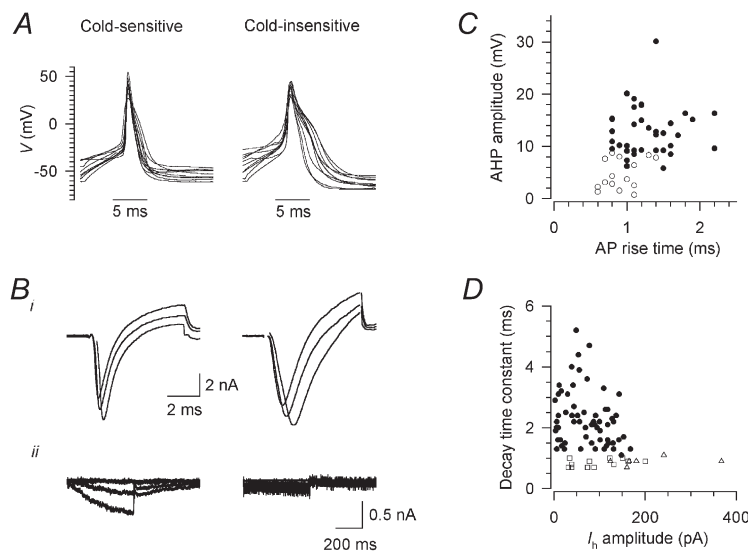
Figure 3. Action potentials and current signatures in cold-sensitive and cold-insensitive neurones

A, action potentials in 10 randomly selected cold-sensitive neurones (left) and 10 cold-insensitive neurones (right) in response to 5 ms depolarising stimuli, aligned so that the peak occurs at the same time. Resting potentials were between −40 and −70 mV; in some cases the beginning of the stimulus is beyond the left edge of the trace. *Bi*, transient inward currents in one cold-sensitive (left) and one cold-insensitive neurone (right); from a holding potential of −60 mV, after a 150 ms prepulse to −80 mV, the potential was stepped to −10, 0 and +10 mV for 6 ms. The decay time constant was measured for the most positive pulse. *Bii*, hyperpolarisation-activated current I_h in one cold-sensitive (left) and one cold-insensitive neurone (right); from a holding potential of −60 mV, the potential was stepped to −70, −90 and −110 mV for 500 ms. Current amplitude was measured for the most negative pulse. Whole-cell (not perforated-patch) recordings, K_2SO_4 pipette solution; recordings were corrected offline for leak and capacitive transients, and any residual capacitive transients are blanked. *C*, relation between action potential rise time and the amplitude of the after-hyperpolarisation (AHP) in cold-sensitive (○) and cold-insensitive (●) neurones. *D*, relation between I_h amplitude and decay time constant of the transient inward current (see *B*) in cold-insensitive neurones (●) and cold-sensitive neurones sensitive (□) and insensitive (△) to capsaicin.

distinguishing cold-sensitive from cold-insensitive neurones were a prominent hyperpolarisation-activated cation current (I_h), rapid decay of transient inward current (determined both by Na^+ current inactivation and K^+ current activation), and a lower degree of expression of a fast-inactivating A-type K^+ current, identified as a transient outward current at 0 mV inactivating with a time constant of less than 50 ms (Table 2 and Fig. 3*B*). Cold-sensitive neurones were closely similar to a previously identified group of neurones (group 3 of Cardenas *et al.* 1995 and Petruska *et al.* 2000*b*; see Discussion). Cold-sensitive and -insensitive neurones were clearly separated by two parameters: AHP amplitude (Fig. 3*C*) and decay time constant of the transient inward current (Fig. 3*D*).

It has been suggested that cold- and capsaicin-sensitive neurones are a subtype of polymodal nociceptor (McKemy *et al.* 2002; Viana *et al.* 2002). Because the action potential configuration and current signatures of nociceptors have been well characterised (Djouhri *et al.* 1998; Petruska *et al.* 2000*b*), we tested whether these parameters in cold- and capsaicin-sensitive neurones are more similar to those of nociceptors, or to those of other cold-sensitive neurones. Of 21 cold-sensitive neurones tested with 1 μM capsaicin for 20 s, 14 responded with an inward current > 50 pA. Both capsaicin-sensitive and -insensitive neurones had current signatures consistent with the previously identified group 3 (see above) although there were slight differences: capsaicin-sensitive neurones had significantly smaller I_h amplitudes, and action potentials of significantly shorter

duration, than capsaicin-insensitive neurones (Table 2; see also Fig. 3*D*). Compared to cold-insensitive neurones, most of which in this size range are capsaicin-sensitive nociceptors (Babes *et al.* 2002), significantly fewer cold- and capsaicin-sensitive neurones showed an inflection during repolarisation (3/14 with inflection compared with 27/38; $P < 0.01$, χ^2 test). We conclude that action potential characteristics and voltage-gated currents in cold- and capsaicin-sensitive neurones differ only slightly from those of other cold-sensitive neurones but are clearly distinct from those found in nociceptors (see Discussion).

Origin of the cold-induced calcium signal

In 22 cold-sensitive neurones the cold stimulus was repeated 2–3 times with a recovery period of at least 5 min between stimuli. The responses to the first and second stimulus were the same ($\Delta F/F_0$: first 0.36 ± 0.20, second 0.36 ± 0.24, $P = 0.90$; threshold: first 29.8 ± 3.4°C, second 30.2 ± 3.0°C, $P = 0.19$; paired *t* test, $n = 22$). Removal of extracellular Ca^{2+} and addition of 1 mM EGTA reduced $\Delta F/F_0$ on cooling in nine cold-sensitive neurones by 95 % (control $\Delta F/F_0 = 0.43 \pm 0.14$; Ca^{2+}-free $\Delta F/F_0 = 0.021 \pm 0.044$, $n = 9$; Fig. 4*Ai*), reducing it to the same level as in cold-insensitive neurones ($P = 0.36$, unpaired *t* test). Removal of extracellular Ca^{2+} also abolished the response to menthol completely ($n = 9$, Fig. 4*Aii*).

We investigated the source of this cold-induced Ca^{2+} entry. To determine to what extent it depends on depolarisation, and how much is attributable to voltage-independent
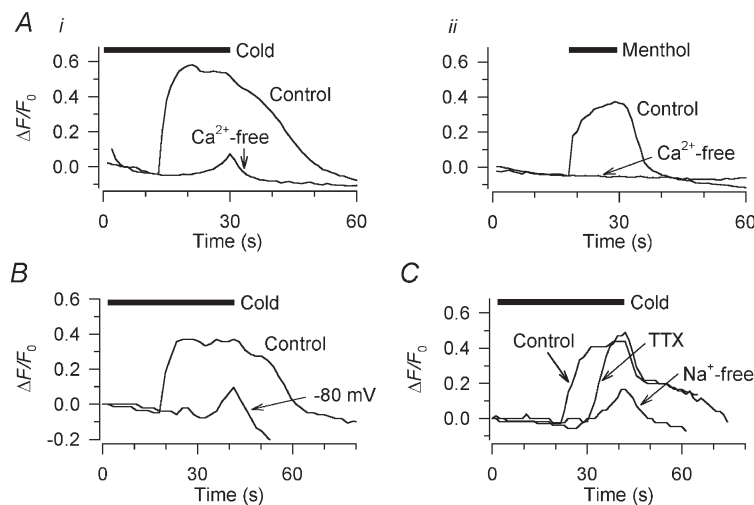
Figure 4. Source of the cold- and menthol-induced rise in [Ca^{2+}]$_i$ in rat DRG neurones

Ai, the cold-induced increase in [Ca^{2+}]$_i$ was abolished in Ca^{2+}-free extracellular solution containing 1 mM EGTA; the cold stimulus here (horizontal bar) was a ramp from 32 to 18 °C without the usual pre-warming step (see Methods). *Aii*, in the same neurone, the increase in [Ca^{2+}]$_i$ elicited by 10 μM (−)-menthol was also abolished by removing extracellular Ca^{2+}. *B*, in a different neurone, the cold-induced rise in [Ca^{2+}]$_i$ was strongly reduced by voltage clamping at −80 mV. The cold stimulus here (horizontal bar) and in all other figures except Fig. 4*A* was the standard one shown in Fig. 1*D*. *C*, in a third neurone, the effects on the cold-induced [Ca^{2+}]$_i$ increase of 1 μM tetrodotoxin (TTX) and of a Na^+-free extracellular solution (*N*-methyl-D-glucamine used as Na^+ substitute) are shown. Three successive cold stimuli were applied, 5 min apart.

entry of Ca^{2+} through a cold-activated Ca^{2+}-permeable channel, we applied a cooling stimulus to six neurones while voltage clamping at -80 mV. This reduced the cold-induced $[Ca^{2+}]_i$ signal by 65 % (current clamp, $\Delta F/F_0 = 0.52 \pm 0.30$; voltage clamp, $\Delta F/F_0 = 0.14 \pm 0.078$, $n = 6$), and there was no longer a distinct threshold for the $[Ca^{2+}]_i$ increase (Fig. 4*B*). The remaining cold-induced $[Ca^{2+}]_i$ signal was significantly larger ($P = 0.015$, unpaired t test) than that recorded in Ca^{2+}-free extracellular solution; we conclude that some voltage-independent Ca^{2+} entry takes place on cooling, but the greater part of the Ca^{2+} entry depends on depolarisation.

We tested to what extent the depolarisation depends on Na^+ ions by cooling 13 cold-sensitive neurones in Na^+-free external solution, with Na^+ replaced by *N*-methyl-D-glucamine (NMDG). The effect of this was indistinguishable from that of voltage clamping at -80 mV (Fig. 4*C*); there was a 73 % reduction in $\Delta F/F_0$ on cooling (control, 0.42 ± 0.18; Na^+-free 0.12 ± 0.12, $n = 13$), and the threshold of the $[Ca^{2+}]_i$ rise became indistinct. We conclude that it is a Na^+-dependent depolarisation that triggers the bulk of the Ca^{2+} influx on cooling.

In 14 cold-sensitive neurones we tested the role of action potential activity in causing voltage-gated Ca^{2+} entry, by applying 1 μM tetrodotoxin (TTX) which abolishes action potentials (see below). The peak $\Delta F/F_0$ on cooling was little altered by this manoeuvre (control, 0.41 ± 0.16; TTX, 0.42 ± 0.20, $n = 14$), but TTX shifted the threshold significantly towards cooler temperatures (control, $31.0 \pm$

4.9 °C; TTX 27.2 ± 3.2 °C, $P = 0.002$, $n = 14$; Fig. 4*C*); this suggests that action potential activity normally sets the threshold temperature for the $[Ca^{2+}]_i$ increase, but that another process is responsible for a large fraction of Na^+-dependent Ca^{2+} entry. We will show below that the cold- and menthol-activated inward current can account for this, because the current is mainly carried by Na^+ ions.

Cold and menthol depolarise cold-sensitive neurones, induce action potentials, and activate an inward current

Neurones identified as cold sensitive by their $[Ca^{2+}]_i$ response to cooling were investigated further using the amphotericin perforated-patch variant of whole-cell recording. We have already described the cold-induced depolarisation and the cold- and menthol-activated current in a separate series of DRG neurones (Reid & Flonta, 2001*a*); our findings in the present study were closely similar and are described briefly here and in Table 3.

Cooling to 18 °C induced a profound depolarisation in all cold-sensitive neurones tested, accompanied in every case by action potentials (Fig. 5*A*); the action potentials were abolished in all 18 neurones by 1 μM TTX and in most by 100 nM TTX (Fig. 5*B*). Simultaneous recordings of membrane potential and $[Ca^{2+}]_i$ confirmed the conclusion reached in the previous section that the threshold of the $[Ca^{2+}]_i$ response is determined by the onset of action potential activity in the absence of TTX (Fig. 5*A*); the $[Ca^{2+}]_i$ response was delayed when action potentials were abolished by TTX (Fig. 5*B*).
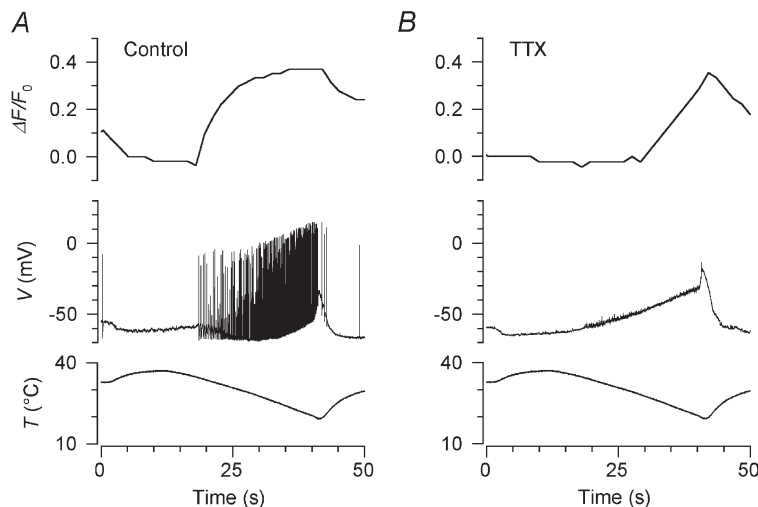
Figure 5. Cold-induced depolarisation and its relation to the $[Ca^{2+}]_i$ signal

A, simultaneous recording of the cold-induced $[Ca^{2+}]_i$ signal (top trace) and membrane potential (middle trace) during the temperature stimulus shown in the bottom trace. The threshold temperatures for action potential activity and the increase in $[Ca^{2+}]_i$ were the same. *B*, recording in the same neurone 5 min later during application of 100 nM TTX, which completely abolished action potential activity. The $[Ca^{2+}]_i$ increase was delayed and threshold was shifted to a lower temperature than in *A*. Unusually, this neurone was firing action potentials at the base temperature of 32 °C before TTX application, and the resting $[Ca^{2+}]_i$ was also relatively high, falling rapidly as the action potentials were shut off by warming (see *A*). For this reason the baseline fluorescence intensity (F_0) for the calculation of $\Delta F/F_0$ in *A* was measured 5 s after the start of the stimulus instead of just before the stimulus as was usual.

	Control	*n*	10 μM (−)-menthol	*n*	100 μM (−)-menthol	*n*	100 μM (+)-menthol	*n*
Resting potential at 32 °C (mV)	−53.2 ± 6.8	48	−56.9 ± 6.8	17	−46.9 ± 7.4 **	9	—	—
Membrane potential at 37 °C (mV)	−54.9 ± 7.1	47	−58.3 ± 7.6	17	−57.4 ± 6.5	9	—	—
Cold-induced depolarisation at 18 °C (mV)	28.9 ± 8.1	45	42.7 ± 10.1 *	17	49.7 ± 6.2 **	9	—	—
Depolarisation threshold (°C)	31.9 ± 5.9	46	33.3 ± 1.9 *	17	36.0 ± 0.9 **	9	—	—
Cold-activated current at 18 °C (pA)	137 ± 90	63	440 ± 395 *	23	746 ± 440 **	35	708 ± 416	9
Cold-activated current threshold (°C)	31.5 ± 2.7	61	34.0 ± 2.6 *	23	37.1 ± 1.6 **	35	35.4 ± 2.1 ***	9

Table 3. Cold- and menthol-induced depolarisation and current in cold-sensitive DRG neurones

* P < 0.01 from control; ** P < 0.01 from 10 μM (−)-menthol; *** P < 0.01 from 100 μM (−)-menthol; Student's paired t test.
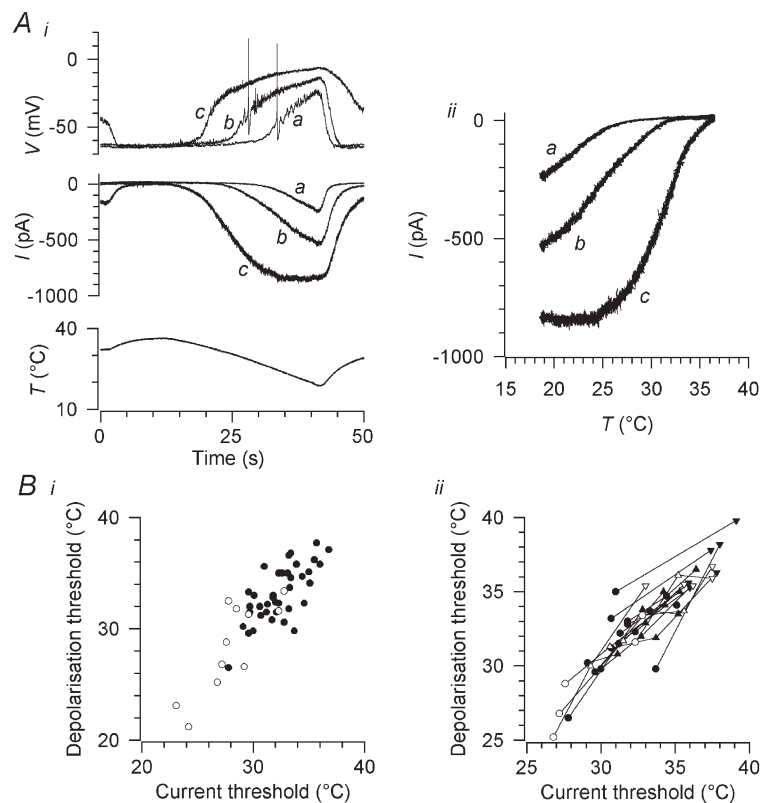
A clear threshold temperature for the cold-induced depolarisation could be determined in most cases (see Fig. 6*A*): during the thermal stimulus, the membrane potential initially showed no change or else a slight, gradual depolarisation with a near-linear relation to the thermal stimulus, and threshold was defined as the first deviation from this trajectory that clearly exceeded the noise level. Application of 10 μM or 100 μM (−)-menthol significantly increased the amplitude of the depolarisation and shifted the threshold temperature significantly towards warmer temperatures (Fig. 6*Ai* and Table 3). In addition, 100 μM (−)-menthol depolarised the resting potential by up to 20 mV; this depolarisation was abolished on warming to 37 °C (Fig. 6*Ai*).

In 61 of 63 cold-sensitive neurones, a cold-activated inward current was present at a holding potential of −60 mV (Table 3 and Fig. 6*Ai*); in the two neurones in which cold did not activate an inward current, application of 100 μM menthol induced a cold-sensitive inward current (not shown). No cold-activated current was found in any of 61 neurones classified as insensitive to cooling based either on the lack of a $[Ca^{2+}]_i$ response to cold or on the lack of depolarisation or action potentials on cooling. In 40 of these neurones, cooling in the presence of 100 μM (−)-menthol also failed to elicit any inward current (not shown). In all neurones tested, the cold-activated current was potentiated in a dose-dependent manner by (−)-menthol, with 10 μM (*n* = 23) and 100 μM (−)-menthol (*n* = 35) reversibly shifting the threshold temperature (defined in a similar way to the depolarisation threshold temperature) towards warmer temperatures and increasing the amplitude of the current (Table 3 and Fig. 6*A*). The action of menthol on membrane potential and membrane current was rapidly and completely reversible (complete washout in 30–40 s).

Figure 6. Cold-induced depolarisation and inward current, and threshold shift caused by menthol

Ai, top, cold-induced depolarisation in the presence of 100 nM TTX (*a*), and its sensitization by 10 μM (*b*) and 100 μM (*c*) (−)-menthol . Middle, cold- and menthol-induced currents in the same neurone at a holding potential of −60 mV; the letters *a*–*c* have the same meanings as in the top panel. Note that 100 μM (−)-menthol depolarised the neurone and activated a current at the base temperature of 32 °C; these effects were reversed by warming to 37 °C. Bottom, the thermal stimulus. *Aii*, the currents in *Ai* during the falling phase of the temperature ramp (10–42 s), plotted against stimulus temperature. *Bi*, threshold temperatures of the cold-induced depolarisation and inward current in 38 neurones cultured in the presence of 50 ng ml⁻¹ nerve growth factor (NGF) (●) and in 11 neurones cultured without NGF (○). *Bii*, shift in current and depolarisation thresholds from control values (●,○) induced by 10 μM (▲,△) and 100 μM (−)-menthol (▼,▽) in 16 neurones cultured with NGF (filled symbols) and five cultured without NGF (open symbols).

The cold- and menthol-activated current normally sets the threshold temperature for depolarisation

The threshold temperatures for the inward shift in current and for the onset of depolarisation during a cooling ramp were very similar (Fig. 6*Bi*). An inward shift in total membrane current may reflect the summed effects of temperature on several ionic currents (including the temperature-sensitive background K^+ current; see Introduction). To isolate more clearly the contribution of the cold- and menthol-activated current to depolarising the neurone, we compared the shifts in current threshold

Figure 7. Stereospecificity of menthol action and modulation of the cold- and menthol-activated current by extracellular Ca^{2+}

A, current–temperature relation of cold- and menthol-activated currents in standard extracellular solution and 100 μM (+)-menthol. Currents in the same neurone in 10 μM and 100 μM (−)-menthol are shown in grey for comparison. Holding potential −60 mV. Action potentials in cell processes are apparent during menthol application. *B*, potentiation of the current by lowered extracellular $[Ca^{2+}]$: the current in 2 mM Ca^{2+}, shown in grey, was increased about twofold by lowering extracellular $[Ca^{2+}]$ to 0.1 mM. *C*, antagonism of the sensitizing effect of (−)-menthol by raised extracellular $[Ca^{2+}]$: the control current, shown in grey, was sensitized by 10 μM (−)-menthol; this sensitization was abolished by raising extracellular $[Ca^{2+}]$ to 10 mM. Holding potential in *B* and *C* was −80 mV.

and depolarisation threshold caused by application of 10 μM and 100 μM (−)-menthol in 21 neurones (Fig. 6*Bii*). The menthol-induced shifts in depolarisation and current threshold were closely similar, indicating that it is a menthol-sensitive current that normally sets the depolarisation threshold of cold-sensitive neurones.

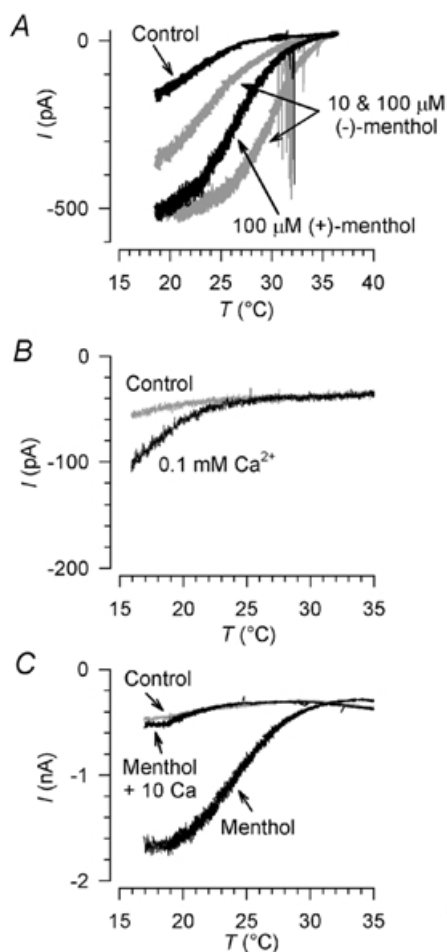### Specificity and stereospecificity of menthol action

To determine whether the action of (−)-menthol is a specific one attributable to binding to a menthol receptor, as distinct from a non-specific alcohol action on the cell membrane or on ion channels in the membrane, we tested the effects of two related compounds on the cold-activated current. The cyclic alcohol cyclohexanol, on which menthol (2-isopropyl-5-methyl-cyclohexanol) is based, was without effect on four cold-sensitive neurones: no current was induced at 32 °C by 100 μM cyclohexanol, and the cold-activated current was not altered (not shown). In addition, we tested the stereoisomer (+)-menthol. At 100 μM, its effect on current amplitude and threshold was intermediate between those of 10 μM and 100 μM (−)-menthol, and the threshold shift was significantly smaller than that induced by 100 μM (−)-menthol (Table 3 and Fig. 7*A*). We conclude that the potentiation by menthol is specific to menthol and not a general alcohol effect, and that its effects show stereospecificity, suggesting that it is binding to a specific receptor in the neuronal membrane.

Modulation by extracellular Ca^{2+}

Cold receptors are known to be strongly influenced by extracellular Ca^{2+} ions. Lowering extracellular $[Ca^{2+}]$ *in vivo* (by infusion of EDTA) or in isolated perfused preparations strongly increases the activity of cold receptors, while raising $[Ca^{2+}]$ antagonises the actions of menthol on spike frequency and burst firing pattern (Hensel & Schäfer, 1974; Schäfer *et al.* 1982; Schäfer *et al.* 1986; Schäfer, 1987). We tested whether these effects are mediated by actions of calcium on the cold- and menthol-activated current. Lowering extracellular $[Ca^{2+}]$ to 0.1 mM increased the current amplitude by 119 ± 53 % ($n = 7$) and shifted the threshold towards warmer temperatures by 2.1 ± 2.0 °C (Fig. 7*B*). The menthol-induced sensitisation of the cold-activated current was abolished by 10 mM extracellular Ca^{2+} ($n = 6$; Fig. 7*C*). The effects of high or low external $[Ca^{2+}]$ on intact cold receptors can thus be accounted for by effects on the cold- and menthol-activated current.

The cold- and menthol-activated current is carried mainly by Na^+ ions

Evidence from $[Ca^{2+}]_i$ imaging (see above) suggests that voltage-independent entry of Ca^{2+} through a Ca^{2+}-permeable channel accounts for a small fraction of total Ca^{2+} entry on cooling, while most of it depends on Na^+ induced depolarisation, a large part of which is independent of action potential activity. We wanted to test to what extent this Na^+-dependent depolarisation could

depend on current through the cold- and menthol-activated channel. The cloned cold and menthol receptor shows similar or higher permeability to Ca^{2+} than to monovalent ions (McKemy *et al.* 2002; Peier *et al.* 2002) and similar findings have been reported in native TG and DRG (McKemy *et al.* 2002; Okazawa *et al.* 2002), but permeability ratios determined using reversal potentials are not a reliable guide as to how much current is carried by each ion under physiological conditions. We therefore measured the effect on the cold-activated current of removing Na^+ ions.

We used NMDG ($n = 6$; 3 perforated-patch, 3 conventional whole-cell recordings using K_2SO_4 pipette solution), tetramethylammonium (TMA; $n = 3$; 2 perforated-patch, 1 conventional whole-cell recording using K_2SO_4 pipette solution) and choline ($n = 2$, both perforated patch) as Na^+ substitutes. When NMDG was substituted for Na^+, the cold-induced depolarisation was greatly reduced (Fig. 8*A*) and the cold-activated current at -80 mV was reduced by $86 \pm 16\%$ ($n = 6$; Fig. 8*B*). Similar results were obtained with choline ($58 \pm 3\%$ reduction in current). This indicates that the greater part of the current through the cold- and menthol-activated channel is carried by Na^+ ions under physiological conditions, and confirms that the cold-induced depolarisation depends primarily on Na^+ influx. Interestingly, when TMA was substituted for Na^+, the cold-activated depolarisation (Fig. 8*A*) and current (Fig. 8*B*) were only slightly reduced, although action potentials were abolished as would be expected owing to the impermeability of voltage-gated Na^+ channels to TMA (Hille, 1992). TMA thus appears to be a permeant ion in the cold- and menthol-activated channel.

The nature of adaptation: a shift in temperature sensitivity induced by increased $[Ca^{2+}]_i$

During long cooling pulses (~5 min), as previously shown (Reid & Flonta, 2001*a*), the cold- and menthol-activated current adapted almost completely with a time constant of

71.5 ± 28 s in the absence of menthol ($n = 10$; Fig. 9*Ai*) and 70.5 ± 46 s in the presence of 100 μM $(-)$-menthol ($n = 6$; not shown).

Desensitisation of capsaicin- and menthol-induced currents in DRG and TG neurones is reported to depend on extracellular Ca^{2+} (Koplas *et al.* 1997; McKemy *et al.* 2002). We tested whether this is also the case for adaptation of cold-activated currents by applying long cooling pulses (270 s, 10–12 °C) in the presence and absence of extracellular Ca^{2+}. Simply omitting Ca^{2+} from the bath solution caused recordings to become unstable, so where Ca^{2+}-free solutions were used we increased extracellular $[Mg^{2+}]$ to 10 mM in both the control and Ca^{2+}-free conditions; in normal (2 mM) extracellular $[Ca^{2+}]$, 10 mM Mg^{2+} slightly reduced the cold-induced current, but did not change the time course of its adaptation. On removing extracellular Ca^{2+} (without adding EGTA, which would chelate Mg^{2+}), adaptation was either abolished or substantially inhibited ($n = 3$, Fig. 9*Ai*).

Adaptation of the cold- and menthol-activated channel is absent in excised patches (Reid & Flonta, 2002), implying that the adaptation mechanism depends on the cellular environment and is not contained within the channel itself. We therefore suspected that a rise in $[Ca^{2+}]_i$ may be the initial signal triggering adaptation. We tested this using the conventional variant of whole-cell patch clamping, instead of the perforated-patch method used in most experiments, including 10 mM BAPTA in the pipette solution to chelate Ca^{2+} ions entering the neurone during cooling; the bath solution was the standard extracellular solution without added Mg^{2+}. In three neurones recorded with BAPTA-containing pipette solution and exposed to long cooling pulses (12 °C, 270 s), adaptation was abolished in one, and substantially slowed in the other two (time constant of 164 ± 104 s, $n = 2$, compared to 71.5 ± 28 s in the perforated-patch experiments; $P = 0.02$, unpaired *t* test; Fig. 9*Aii*). In two neurones recorded with

Figure 8. Dependence of the cold-induced depolarisation and inward current on external Na^+

A, effects of two Na^+ substitutes on cold-induced depolarisation. Three cold stimuli were applied at intervals of 4.5 min, in the following order: control (top trace), *N*-methyl-D-glucamine (middle trace, NMDG), tetramethylammonium (middle trace, TMA). *B*, in the same neurone, replacement of Na^+ by NMDG strongly inhibited the cold-activated inward current while a substantial current was present in TMA. Holding potential was -60 mV.
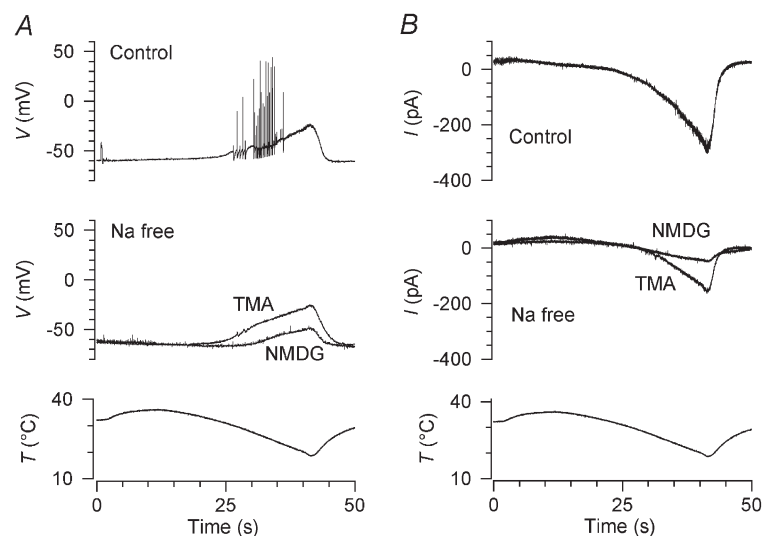
10 mM EGTA, a slower Ca^{2+} chelator, the time course of adaptation was not different from that recorded in the perforated-patch configuration (86.9 ± 31 s, $P = 0.50$; not shown).

We hypothesised that adaptation could involve two possible processes: the temperature sensitivity of the current could be shifted, so that stronger cooling is required to activate a given current but maximum current is not altered; or the available number of ion channels could be reduced, leading to a fall in maximum current

without a change in temperature sensitivity. We therefore tried to distinguish whether temperature sensitivity changes as adaptation proceeds.

In nine neurones recorded in standard extracellular solution, we compared the current–temperature relation during falling and rising temperature ramps; in every case, the current during the rising ramp was shifted towards colder temperatures compared with the falling ramp (see the first ramp *a* in Fig. 9*B*). To exclude a simple dependence on the direction of the temperature ramp, we added a second pair of ramps in a further five neurones
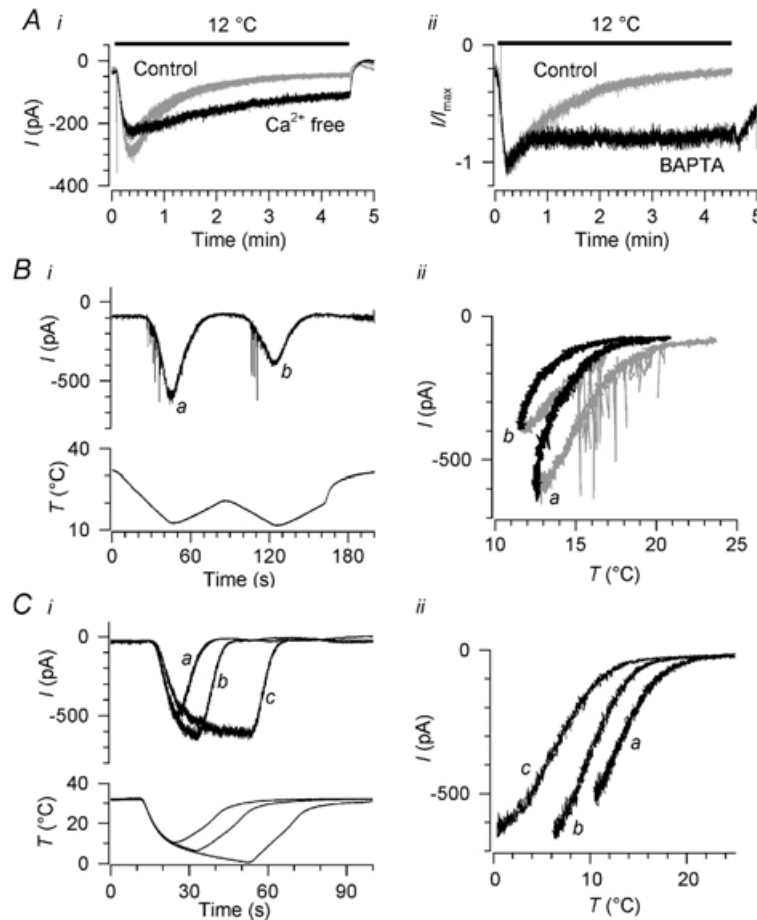
Figure 9. Adaptation of the cold- and menthol-activated current: time course, Ca^{2+} dependence and shift in temperature sensitivity

Ai, time course of adaptation on cooling and the effect of removing extracellular Ca^{2+}. Three pulses to 12 °C were applied, separated by 5 min, the second one (black) being in Ca^{2+}-free extracellular solution and the first and third (grey) in normal $[Ca^{2+}]$. Extracellular $[Mg^{2+}]$ was raised to 10 mM throughout. *Aii*, the effect on adaptation time course of including 10 mM BAPTA in the pipette solution, recorded in two different neurones in standard extracellular solution. The control recording was in the perforated-patch configuration and was chosen because its adaptation time constant (69 s) was close to the mean for all perforated-patch recordings (71.5 s). Currents are normalised; peak currents were ~200 pA (BAPTA) and ~500 pA (control). *B*, shift in the temperature sensitivity of the cold-activated current during successive falling and rising temperature ramps, in standard extracellular solution; *i,* raw currents and temperature stimulus, and *ii,* current–temperature relationship. Falling temperature ramps are shown in grey in *ii*, and rising ramps in black; the two pairs of ramps are marked *a* and *b* for easy identification. *C*, effect of cooling pulses of duration 10, 20 and 40 s on the temperature dependence of the cold-activated current, measured during rising ramps (*a–c*) following each cold pulse, in standard extracellular solution. *i,* raw currents; *ii,* current–temperature relationship, showing only currents during the rising ramps *a–c*. Holding potential was −60 mV in *A–C*.

(*b* in Fig. 9*B*). Comparing the current–temperature relationship of the second rising ramp with that of the first, a parallel shift towards lower temperatures is evident. We also applied rising temperature ramps at different times during a cold pulse (Fig. 9*Ci*), comparing the current–temperature relationship during rising temperature ramps after cold pulses of 10–40 s duration, each separated by a recovery period of at least 3 min. The current was again shifted towards lower temperatures and the extent of the shift depended on the duration of the cold pulse and the degree of cooling (*n* = 4; Fig. 9*Cii*).

We tested whether this shift in temperature sensitivity could be induced by artificially raising $[Ca^{2+}]_i$ by applying 1 min trains of depolarising pulses to two cold-sensitive neurones at 32 °C, during the interval between two cooling ramps (Fig. 10). The rise in $[Ca^{2+}]_i$ during the pulse train in Ca^{2+}-containing extracellular solution was similar to that during the standard cold stimulus ($\Delta F/F_0 = 0.49$ and 0.45), while $[Ca^{2+}]_i$ did not change at all in Ca^{2+}-free extracellular solution. The cooling ramps were applied 2 min apart, which we had previously established is sufficient time for recovery of the current between cold stimuli in voltage clamp mode. In both neurones in 2 mM extracellular $[Ca^{2+}]$ (with 10 mM Mg^{2+}), the current during the second cooling ramp was reduced (by 44 and 81 % respectively)

and shifted towards colder temperatures (by 2.5 °C in each case), indicating that the pulse train had induced adaptation; this shift was reversible after 5 min (Fig. 10*Bi*). In the same neurones, removing Ca^{2+} from this solution (without adding EGTA) prevented the shift (Fig. 10*Bii*), indicating that the adaptation was not caused by the depolarising pulses but by the resulting Ca^{2+} influx. We conclude that a rise in $[Ca^{2+}]_i$ similar to that occurring on cooling is sufficient to trigger cold adaptation, by shifting the temperature sensitivity of the cold- and menthol-activated current.

Cross-adaptation by capsaicin-activated current

Given the apparent similarity between adaptation of the cold-activated current and desensitisation of capsaicin-activated currents, we were curious to know whether cold adaptation could be induced by capsaicin application. We therefore tested the effect of 20–60 s capsaicin application on 19 cold-sensitive neurones. Twelve of the neurones were capsaicin-sensitive (current 1.3 ± 1.6 nA in response to 0.5 μM capsaicin) and in 11 of these (7 perforated-patch, 4 conventional whole-cell recordings with K_2SO_4 pipette solution) we were able to apply cooling stimuli immediately after the capsaicin-induced current had returned to baseline (~2 min after the application). In all 11 neurones the cold-activated current was profoundly inhibited, with
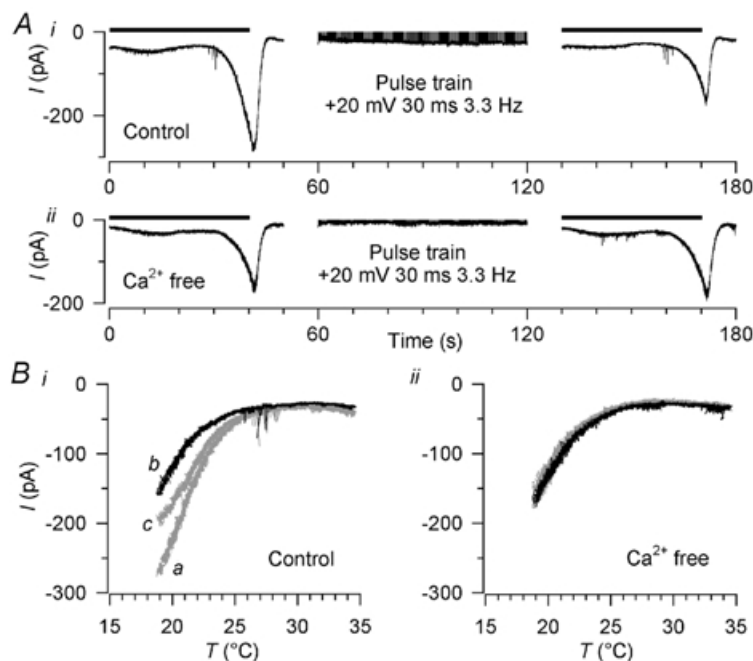

Figure 10. Induction of adaptation by raised $[Ca^{2+}]_i$

A, induction of adaptation by raising $[Ca^{2+}]_i$ with trains of depolarising pulses. *Ai*, a cooling stimulus of the standard type (horizontal bar; see Fig. 1*D*) was followed immediately by a 1 min train of depolarising pulses (to +20 mV for 30 ms at 300 ms intervals) and then another cooling stimulus (horizontal bar); the cold-activated current was reduced after the pulse train. *Aii*, in the same neurone in Ca^{2+}-free extracellular solution, the cold-activated current was unchanged by the pulse train. Extracellular $[Mg^{2+}]$ was raised to 10 mM throughout. *B*, current–temperature relationship of the currents in *A*. Cold-activated currents before the pulse train are shown in grey and marked *a* in *i*; currents immediately after the pulse train are in black and marked *b* in *i*. In addition, currents 5 min after the pulse train are plotted; these are in grey and marked *c* in *i*. Holding potential was −60 mV.

the threshold being shifted by 10.2 ± 4.6 °C towards cooler temperatures ($n = 11$; Fig. 11*A*). In five of these 11 neurones no cold-activated current was detectable at the minimum stimulus temperature of 18 °C. In these cases the threshold was assumed to be 18 °C for the purposes of calculating the threshold shift, which is therefore a minimum estimate of the true change in threshold. The shift in threshold correlated significantly with the amplitude of the capsaicin-induced current ($r = 0.80$, $P = 0.003$, Fig. 11*Aii*), with no difference being observable between perforated-patch and conventional whole-cell recordings. This inhibition was slowly reversible. In contrast, in capsaicin-insensitive neurones, capsaicin application had no effect on the cold-activated current; this was true whether cooling was applied immediately after washing off capsaicin ($n = 5$ of 7 capsaicin-insensitive neurones) or in the continued presence of capsaicin ($n = 2$). We conclude that the activation of an inward current by capsaicin (but not capsaicin itself) induces cross-adaptation (or cross-desensitisation) to subsequent cooling stimuli.

Modulation of cold sensitivity by nerve growth factor

Regulation by nerve growth factor (NGF) of the cold- and menthol-activated current would be plausible given the recent observation that mRNA for the cloned cold and menthol receptor is present in neurones expressing the high-affinity NGF receptor TrkA (Peier *et al.* 2002) and the importance of NGF in the regulation of the capsaicin receptor VR-1 (Bevan & Winter, 1995; Shu & Mendell, 2001; Winston *et al.* 2001). To test whether NGF modulates cold sensitivity and alters the properties of the cold- and menthol-induced current, we cultured DRG neurones in the absence of NGF (7 cultures) and compared the cold-induced $[Ca^{2+}]_i$ signal and cold-induced depolarisation with neurones cultured under our normal conditions with NGF (21 cultures). Two of the seven cultures were 'split', culturing half the coverslips with and half without, NGF as an internal control. We measured changes in $[Ca^{2+}]_i$ induced by cooling alone or by a combination of 100 μM ($-$)-menthol and cooling, and also measured cold-induced depolarisation and cold-induced inward current.
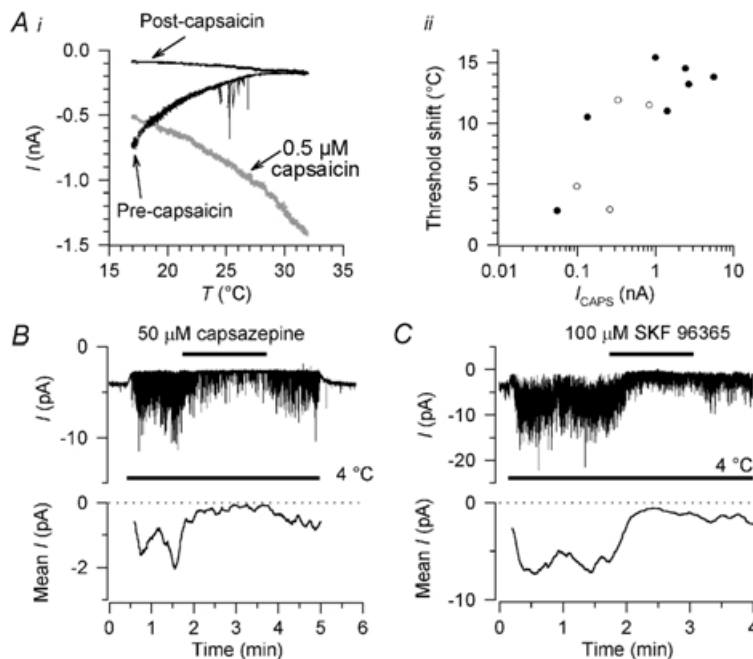
Figure 11. Cross-adaptation caused by capsaicin-induced current and block by capsazepine and SKF 96365

Ai, application of 0.5 μM capsaicin for 1 min induced adaptation of the cold-activated current in a capsaicin-sensitive neurone; current activated by capsaicin is shown in grey. Holding potential was -60 mV. *ii*, correlation between the shift in threshold after capsaicin application and the amplitude of the capsaicin-induced current (I_{CAPS}) in 11 cold-sensitive neurones, seven recorded in perforated-patch ($\bullet$) and four in conventional whole-cell configuration ($\circ$). Capsaicin-induced current amplitude is shown on a logarithmic scale because of the wide range of values. In neurones like that in *A*, where an 18 °C stimulus no longer elicited a cold-activated current, the threshold was assumed to be 18 °C for the purposes of calculating the threshold shift shown here. *B*, block of cold-activated channel activity by 50 μM capsazepine in a multi-channel outside-out patch, and recovery on washout. *C*, block of cold-activated channel activity by 100 μM SKF 96365 in another multi-channel outside-out patch, with slow and partial recovery on washout. Holding potential in *B* and *C* was -80 mV. Mean current traces (lower traces) are moving averages over 10 s of activity, corrected for leak at 4 °C; only the periods at 4 °C are shown in the mean current traces.

Table 4. Effects of nerve growth factor on cold responsiveness and the cold-activated current

	NGF	n	no NGF	n	$P*$
$\Delta F/F_0$ on cooling	0.40 ± 0.16	205	0.33 ± 0.16	50	0.007
Threshold temperature for increase in $[Ca^{2+}]_i$ (°C)	30.5 ± 3.8	205	27.9 ± 3.5	50	< 0.001
Threshold temperature for increase in $[Ca^{2+}]_i$ in 100 μM (−)-menthol (°C)	35.4 ± 4.0	26	29.9 ± 8.0	12	0.008
Cold-induced depolarisation at 18 °C (mV)	28.9 ± 8.1	45	20.4 ± 8.3	16	< 0.001
Depolarisation threshold (°C)	31.9 ± 5.9	46	28.3 ± 3.8	13	0.04
Cold-activated current at 18 °C (pA)	137 ± 90	63	60 ± 52	15	0.002
Cold-activated current threshold (°C)	31.5 ± 2.7	62	28.6 ± 2.9	13	< 0.001

* Student's unpaired t test.

The $[Ca^{2+}]_i$ increase on cooling was larger in cold-sensitive neurones cultured with 50 ng ml^{-1} NGF 7S than without NGF, and the threshold was at a higher temperature (Table 4). In the 'split' cultures, we measured the threshold temperature of the cold-induced $[Ca^{2+}]_i$ increase in the presence of 100 μM (−)-menthol; a similar significant difference was evident between neurones cultured with, and without NGF. The cold-induced depolarisation was larger in neurones cultured with NGF, and the depolarisation began at a higher temperature (Fig. 6*B*). The cold-activated inward current was over twice as large in neurones cultured with NGF than without, and its threshold was about 3 °C warmer (Table 4 and Fig. 6*B*). The change in current threshold or amplitude induced by menthol was not altered by NGF (not shown), nor did NGF change the proportion of cold-sensitive neurones (NGF, 67/923, 7.3 %; no NGF, 21/297, 7.1 %).

We conclude that NGF increases the amplitude of the cold- and menthol-sensitive current and makes it more sensitive to cooling, but that it does not induce expression of the current in neurones not already expressing it.

Inhibition of the cold- and menthol-activated channel by capsazepine and SKF 96365
After the cloning of the cold and menthol receptor revealed that it is a member of the transient receptor potential (TRP) family, we tested known blockers of TRP channels – lanthanum (Clapham *et al.* 2001), SKF 96365 (Mori *et al.* 2001) and capsazepine, which blocks the capsaicin receptor VR1 (Bevan *et al.* 1992). Lanthanum, at a concentration up to 100 μM, had no effect on the cold-activated current ($n = 2$, not shown). The other compounds inhibited the cold-activated current: 50 μM capsazepine reduced it by 94 ± 15 % ($n = 7$; 1 perforated-patch, 6 conventional whole-cell recordings with K_2SO_4 pipette solution) and 100 μM SKF 96365 reduced it by 68 ± 29 % ($n = 5$; 4 perforated-patch, 1 conventional whole-cell recording with K_2SO_4 pipette solution). The effect of SKF 96365 had a slow onset and extremely slow reversal (incomplete within 10 min). The action of capsazepine was also rather slow but washout was more rapid. We verified in multi-channel excised patches that

these effects were attributable to a direct block of the cold- and menthol-activated channel and not to indirect mechanisms; at the same concentrations as used in whole cell recordings, both drugs blocked channel activity in outside-out patches, implying that both act directly ($n = 5$ for capsazepine, Fig. 11*B*; $n = 3$ for SKF 96365, Fig. 11*C*).

DISCUSSION
The proportion of cold-sensitive neurones found in this study (67/923, 7.3 %) and in an earlier report (45/643, 7.0 %; Reid & Flonta, 2001*a*) is consistent with values reported by others in rat DRG and TG (Suto & Gotoh, 1999; McKemy *et al.* 2002; Viana *et al.* 2002) and with *in vivo* estimates of cold receptor numbers in rat hindlimb (Leem *et al.* 1993*a*; Gee *et al.* 1999). We found cold- and menthol-sensitive neurones to be among the smallest in the DRG (Fig. 1*F*), in agreement with reports on cold-sensitive (Suto & Gotoh, 1999) and menthol-sensitive (Okazawa *et al.* 2000) DRG neurones, and recent findings in TG (Viana *et al.* 2002). The small size and dark soma are consistent with reports that the majority of cold-sensitive fibres in the rat hindlimb *in vivo* are C-fibres (Iriuchijima & Zotterman, 1960; Leem *et al.* 1993*a*; Leem *et al.* 1993*b*). The threshold temperatures we report here suggest a role for these neurones in the detection of innocuous cooling.

Role of the cold- and menthol-activated current in peripheral cold transduction
The parallel shift in the depolarisation and current threshold temperatures on menthol application (Fig. 6*Bii*) implies that the cold- and menthol-activated current normally sets the threshold temperature for depolarisation on cooling. Expression of the current appears to be highly specific to cold-sensitive neurones. It was present in all of 63 cold-sensitive neurones and all of 27 in a previous study (Reid & Flonta, 2001*a*), while it was absent from all of 61 cold-insensitive neurones, 40 of which were cooled in the presence of 100 μM (−)-menthol. Our observation that only 71 % of cold-sensitive neurones reacted to menthol at 32 °C (Results and Table 1) does not imply a lack of expression of the cold- and menthol-activated channel in

some neurones; it can be simply explained by the finding that the apparently menthol-insensitive neurones were those least sensitive to cold (mean threshold 25.6 °C, Table 1). The shift in threshold of ~6 °C induced by 100 μM ($-$)-menthol (Table 3) would therefore not be sufficient to excite these neurones at the base temperature of 32 °C.

The importance of other cold-sensitive mechanisms is suggested by Fig. 6*Ai*. A current of ~200 pA induced by menthol depolarised neurones by ~20 mV (trace *c*), while a current of the same magnitude induced by cold (at about 22 °C) produced a depolarisation nearly twice as large (trace *a*). The simplest explanation for this difference is that it reflects the lower background conductance during cooling due to the inhibition of a cold-sensitive background K$^+$ current (Reid & Flonta, 2001*b*; Viana *et al.* 2002). The mean cold-activated current of 140 pA (Table 3) is small in relation to other transduction currents in native DRG neurones activated by heat (Cesare & McNaughton, 1996), protons (Bevan & Yeats, 1991) and ATP (Cook *et al.* 1997); without a parallel reduction in background membrane conductance, the cold-activated inward current would probably produce a much smaller depolarisation than is observed on cooling.

Turning to intact cold receptors, several aspects of their function are accounted for by the cold- and menthol-activated channel. It can explain the menthol responsiveness of cold receptors, including its sensitisation of their response to cold and the antagonism of its action by warming (Hensel & Zotterman, 1951*a*; Schäfer *et al.* 1986). Low extracellular [Ca^{2+}] stimulates intact cold receptors (Hensel & Schäfer, 1974; Schäfer *et al.* 1982; Schäfer, 1987); this can be accounted for by a potentiation of the cold-activated current (Fig. 7*B*). The stimulatory effect of menthol, and the alterations in burst firing pattern it induces, can be antagonised in intact cold receptors by raised extracellular [Ca^{2+}] (Schäfer *et al.* 1986), which also antagonises the menthol sensitisation of the cold-activated current (Fig. 7*C*). We conclude that the cold- and menthol-activated current can account for all the known effects of menthol and calcium on cold receptors, which have previously been explained by other mechanisms (Schäfer *et al.* 1984; Schäfer *et al.* 1986).

'Current signature' and action potentials

Classification of DRG neurones based on the pattern of expression of voltage-gated currents (the 'current signature'; see Results) is practically useful if one wants to predict the likely functional properties of a neurone being recorded without applying an agonist (e.g. menthol or capsaicin) to that neurone and all others in the culture dish. With small quantitative differences, all cold-sensitive neurones showed properties consistent with a previously identified group, group 3 of Cardenas *et al.* (1995) and Petruska *et al.* (2000*b*). This group is negative for substance P and neurofilament immunoreactivity and for

IB4 binding (Petruska *et al.* 2000*a*; Petruska *et al.* 2000*b*), consistent with a report that neurones expressing mRNA coding for the cold and menthol receptor do not express these functional markers (Peier *et al.* 2002). However, group 3 neurones are reported to be insensitive to capsaicin, whereas we and others find that about half of cold-sensitive neurones respond to capsaicin (see below).

As reported for TG neurones (Viana *et al.* 2002), the amplitude of the hyperpolarisation-activated current I_h was larger in cold-sensitive than cold-insensitive neurones, fewer of them expressed an A-type K$^+$ current, and action potential durations were shorter. There was considerable overlap in I_h amplitude and action potential duration between cold-sensitive and -insensitive neurones (see Table 2) and these measures are thus of limited use for pre-selection. In contrast, two other parameters separated cold-sensitive neurones reliably from cold-insensitive neurones with almost no overlap: the decay of the transient inward current (determined both by Na$^+$ current inactivation and K$^+$ current activation) was more rapid in cold-sensitive than cold-insensitive neurones, and the after-hyperpolarisation after the action potential was smaller or absent (Fig. 3*C* and *D*).

Capsaicin sensitivity

Capsaicin responsiveness in cold-sensitive neurones has also been reported in TG cultures (McKemy *et al.* 2002; Viana *et al.* 2002), and the authors of both studies suggested that these neurones are cold-sensitive polymodal nociceptors and form a separate group from capsaicin-insensitive cold receptors. Our evidence tends against such a clear functional separation, showing a continuum of properties between two extremes (Fig. 2). Capsaicin-sensitive neurones had cold threshold temperatures throughout the range we tested, and all were in the non-noxious range. They are therefore not nociceptors in the usual sense of receptors that respond only to stimuli causing tissue damage or pain (Burgess & Perl, 1967; Bessou & Perl, 1969).

The action potential characteristics of cold- and capsaicin-sensitive neurones are also quite different from those typical of nociceptors: their action potential duration is short, and the number of neurones showing an inflection during repolarisation is small (Table 2; cf. Djouhri *et al.* 1998). Their current signatures were consistent with those of other cold-sensitive neurones but quite different from those of neurones likely to be nociceptors (Petruska *et al.* 2000*b*). The size of cold- and capsaicin-sensitive neurones also suggests that they are not simply a subgroup of poly-modal nociceptor: they were significantly smaller than capsaicin-sensitive neurones in general (a group largely composed of polymodal nociceptors), while they did not differ in size from cold-sensitive neurones that were insensitive to capsaicin (Table 1). For these reasons, as well as their innocuous threshold temperatures, it seems to us premature to suggest that these neurones are a subtype

of polymodal nociceptor solely on the basis of their sensitivity to capsaicin.

Capsaicin sensitivity is probably due to expression of the capsaicin receptor VR-1, which would also make these neurones sensitive to noxious heat (Caterina *et al.* 1997). This could account for the 'paradoxical' discharge induced in some cold receptors by strong heating, which induces a sensation of cold (Dodt & Zotterman, 1952; Long, 1977). The sensitisation of the paradoxical discharge by heat-induced tissue injury (Dubner *et al.* 1975) is reminiscent of the sensitisation of native heat-evoked currents, which are probably generated by VR-1 (Cesare & McNaughton, 1996). It is not obvious what function the co-expression of VR-1 in innocuous cold receptors could have in the normal life of the animal.

Another possibility is that cold receptors do not express VR-1 *in vivo*. To our knowledge, cold-sensitive neurones responding to capsaicin have been described only in primary culture (McKemy *et al.* 2002; Viana *et al.* 2002; this article), whereas the only study to have been carried out in intact DRG found no co-expression of VR-1 with mRNA coding for the cloned cold and menthol receptor (Peier *et al.* 2002). The possibility that co-expression of cold and capsaicin sensitivity is a culture artefact cannot at present be excluded.

Source of the cold-induced $[Ca^{2+}]_i$ signal

Our finding that the $[Ca^{2+}]_i$ increase caused by cold and menthol depends on influx of Ca^{2+} is consistent with previous separate studies in DRG neurones sensitive to cold (Suto & Gotoh, 1999) and to menthol (Okazawa *et al.* 2000). Two previous studies have reached conflicting conclusions on the route of cold-induced Ca^{2+} entry, suggesting that it is independent of Na^+-induced depolarisation (Suto & Gotoh, 1999), or that it is voltage-gated, resulting from Na^+-dependent action potential activity (Viana *et al.* 2002). This latter suggestion is supported by the observation that Cd^{2+} ions, which block voltage-gated Ca^{2+} channels, inhibit the cold-induced $[Ca^{2+}]_i$ signal (Thut & Gold, 2001; Okazawa *et al.* 2002). We conclude that most of the cold-induced Ca^{2+} signal depends on a Na^+-induced depolarisation (Fig. 4*B* and *C*), but that action-potential activity is not the only or major source of the depolarisation-induced Ca^{2+} increase; it depends also on inward Na^+ current through the cold- and menthol-activated channel, whose current is mostly carried by Na^+ ions under physiological conditions (Fig. 8). In addition, we do find evidence of voltage-independent Ca^{2+} entry, although its contribution to the total $[Ca^{2+}]_i$ increase on cooling is a small one; this is consistent with reports of a similar or slightly higher permeability to Ca^{2+} than to monovalent ions (P_{Ca}/P_{Na} 3.3, McKemy *et al.* 2002; P_{Ca}/P_{Na} 0.97, Peier *et al.* 2002) although another study has shown a higher relative Ca^{2+} permeability (P_{Ca}/P_{Na} 8.2, Okazawa *et al.* 2002).

Adaptation

The adaptation process of cold receptors *in vivo* has rapid and slow components. In monkeys and humans, strong adaptation is observed during stimuli as short as 8–10 s (Darian-Smith *et al.* 1973; Campero *et al.* 2001) and adaptation is reported to be nearly complete in 30 s (Kenshalo & Duclaux, 1977). We find that adaptation is first apparent as a rapid shift in temperature sensitivity, occurring within 20 s of the beginning of a cooling stimulus while the temperature is still falling (Fig. 9*C*); this shift is thus likely to be involved in the rapid adaptation of cold receptors *in vivo*. The slower current decline during a long cooling pulse (control traces in Fig. 9*A*) has a similar time course to a slow adaptation process in intact cold receptors (Kenshalo & Duclaux, 1977) and to the adaptation of human cold sensation (Kenshalo, 1970). Our experiments and the *in vivo* reports cited do not exclude the possibility that the rapid and slow adaptation processes are separate.

Adaptation by shifting temperature sensitivity is analogous to the adaptation of the mechanotransduction channel of hair cells, which involves a shift in the force–current relation, preserving the sensitivity of the channel to increments of force (Assad *et al.* 1989). In a similar way, adaptation would preserve the sensitivity of the cold- and menthol-activated channel by shifting its threshold depending on the adapting temperature. We have shown that the process depends strongly on $[Ca^{2+}]_i$: it can be inhibited by the rapid Ca^{2+} chelator BAPTA (Fig. 9*Aii*), in agreement with a very recent report (Okazawa *et al.* 2002), and it can be induced by artificially raising $[Ca^{2+}]_i$ (Fig. 10). As discussed above, Ca^{2+} entry primarily results from the depolarisation induced by the cold- and menthol-activated channel, implying that the channel adjusts its own temperature sensitivity by Ca^{2+}-regulated feedback. As we have shown previously, adaptation is not a feature of the cold- and menthol-activated channel itself: it is absent in excised outside-out patches (Reid & Flonta, 2002), although interestingly Ca^{2+} sensitivity is intact in some inside-out patches (Okazawa *et al.* 2002). The sensitisation of the current by low extracellular $[Ca^{2+}]$ (Fig. 7*B*) may be due to removal of resting adaptation by lowered $[Ca^{2+}]_i$.

The dependence of adaptation on $[Ca^{2+}]_i$ in the cold- and menthol-activated channel is reminiscent of the $[Ca^{2+}]_i$-dependent desensitisation of a related ion channel, the capsaicin receptor VR-1 (Docherty *et al.* 1996; Koplas *et al.* 1997). The possibility that both channels share common mechanisms of adaptation or desensitisation is suggested by our observation of cross-adaptation (Fig. 11*A*), although there is at present no evidence to suggest that the shared mechanisms involve more than a common dependence on $[Ca^{2+}]_i$.

NGF sensitivity and putative blockers

Our observation that NGF sensitises the cold-activated current suggests that in inflammation, along with the

well-studied sensitisation of nociceptors, cold receptors may also be sensitised. TrkA links to a variety of different signalling pathways, some regulating gene expression, others potentially modulating the properties of existing molecules (Kaplan & Miller, 2000; Patapoutian & Reichardt, 2001) including the acute sensitisation of VR-1 (Chuang *et al.* 2001; Shu & Mendell, 2001). We have not tested whether NGF acutely modulates the cold- and menthol-activated current, but the shift in temperature threshold we observe indicates that NGF is altering the properties of individual channels as well as possibly increasing the number of channels expressed.

A blocker for this channel would be useful in investigating its function in intact cold receptors. We have identified two potential compounds, capsazepine and SKF 96365. Both act directly on the cold- and menthol-activated channel (Fig. 11*B* and *C*). However, neither capsazepine nor SKF 96365 is a specific blocker: capsazepine has a well-known action on VR-1, the purpose for which it was developed (Bevan *et al.* 1992), and also affects nicotinic acetylcholine receptors and voltage-gated Ca^{2+} channels (Docherty *et al.* 1997; Liu & Simon, 1997), while SKF 96365 is known to block voltage-gated Ca^{2+} channels (Mori *et al.* 2001). These two compounds may be of limited use in functional studies, but more specific and potent blockers are required.

In conclusion, the cold- and menthol-activated current we describe here accounts for many of the properties of cold receptors *in vivo*, including their adaptation, menthol sensitivity and modulation by calcium. It appears to have a dominant role in setting the threshold temperature for cold-induced depolarisation. The temperature sensitivity of the ion channels underlying it is not fixed, but is shifted by $[Ca^{2+}]_i$-dependent cold adaptation, and the Ca^{2+} entry causing adaptation results from activity of the channels themselves. The current is specific to cold-sensitive neurones within the DRG and, although other temperature-sensitive mechanisms influence cold receptor excitability, it seems likely to be the main cold transduction mechanism.

REFERENCES

Assad, J. A., Hacohen, N. & Corey, D. P. (1989). Voltage dependence of adaptation and active bundle movement in bullfrog saccular hair cells. *Proceedings of the National Academy of Sciences of the USA* **86**, 2918–2922.

Babes, A., Amuzescu, B., Krause, U., Scholz, A., Flonta, M.-L. & Reid, G. (2002). Cooling inhibits capsaicin-induced currents in cultured rat dorsal root ganglion neurones. *Neuroscience Letters* **317**, 131–134.

Baccaglini, P. I. & Hogan, P. G. (1983). Some rat sensory neurons in culture express characteristics of differentiated pain sensory cells. *Proceedings of the National Academy of Sciences of the USA* **80**, 594–598.

Bessou, P. & Perl, E. R. (1969). Response of cutaneous sensory units with unmyelinated fibers to noxious stimuli. *Journal of Neurophysiology* **32**, 1025–1043.

Bevan, S., Hothi, S., Hughes, G., James, I. F., Rang, H. P., Shah, K., Walpole, C. S. & Yeats, J. C. (1992). Capsazepine: a competitive antagonist of the sensory neurone excitant capsaicin. *British Journal of Pharmacology* **107**, 544–552.

Bevan, S. & Winter, J. (1995). Nerve growth factor differentially regulates the chemosensitivity of adult rat cultured sensory neurons. *Journal of Neuroscience* **15**, 4918–4926.

Bevan, S. & Yeats, J. (1991). Protons activate a cation conductance in a subpopulation of rat dorsal root ganglion neurones. *Journal of Physiology* **433**, 145–161.

Braun, H. A., Bade, H. & Hensel, H. (1980). Static and dynamic discharge patterns of bursting cold fibers related to hypothetical receptor mechanisms. *Pflügers Archiv* **386**, 1–9.

Burgess, P. R. & Perl, E. R. (1967). Myelinated afferent fibres responding specifically to noxious stimulation of the skin. *Journal of Physiology* **190**, 541–562.

Campero, M., Serra, J., Bostock, H. & Ochoa, J. L. (2001). Slowly conducting afferents activated by innocuous low temperature in human skin. *Journal of Physiology* **535**, 855–865.

Cardenas, C. G., Del Mar, L. P. & Scroggs, R. S. (1995). Variation in serotonergic inhibition of calcium channel currents in four types of rat sensory neurons differentiated by membrane properties. *Journal of Neurophysiology* **74**, 1870–1879.

Caterina, M. J., Schumacher, M. A., Tominaga, M., Rosen, T. A., Levine, J. D. & Julius, D. (1997). The capsaicin receptor: a heat-activated ion channel in the pain pathway. *Nature* **389**, 816–824.

Cesare, P. & McNaughton, P. (1996). A novel heat-activated current in nociceptive neurons and its sensitization by bradykinin. *Proceedings of the National Academy of Sciences of the USA* **93**, 15435–15439.

Cesare, P. & McNaughton, P. (1997). Peripheral pain mechanisms. *Current Opinion in Neurobiology* **7**, 493–499.

Chuang, H. H., Prescott, E. D., Kong, H. Y., Shields, S., Jordt, S. E., Basbaum, A. I., Chao, M. V. & Julius, D. (2001). Bradykinin and nerve growth factor release the capsaicin receptor from PtdIns(4,5)P$_2$-mediated inhibition. *Nature* **411**, 957–962.

Clapham, D. E., Runnels, L. W. & Strübing, C. (2001). The TRP ion channel family. *Nature Reviews Neuroscience* **2**, 387–396.

Cook, S. P., Vulchanova, L., Hargreaves, K. M., Elde, R. & McCleskey, E. W. (1997). Distinct ATP receptors on pain-sensing and stretch-sensing neurons. *Nature* **387**, 505–508.

Darian-Smith, I. (1984). Thermal sensibility. In *Handbook of Physiology,* Section 1, *The Nervous System*, ed. Darian-Smith, I., pp. 879–913. American Physiological Society, Bethesda, Maryland.

Darian-Smith, I., Johnson, K. O. & Dykes, R. (1973). 'Cold' fiber population innervating palmar and digital skin of the monkey: responses to cooling pulses. *Journal of Neurophysiology* **36**, 325–346.

Djouhri, L., Bleazard, L. & Lawson, S. N. (1998). Association of somatic action potential shape with sensory receptive properties in guinea-pig dorsal root ganglion neurones. *Journal of Physiology* **513**, 857–872.

Docherty, R. J., Yeats, J. C., Bevan, S. & Boddeke, H. W. G. M. (1996). Inhibition of calcineurin inhibits the desensitization of capsaicin-evoked currents in cultured dorsal root ganglion neurones from adult rats. *Pflügers Archiv* **431**, 828–837.

Docherty, R. J., Yeats, J. C. & Piper, A. S. (1997). Capsazepine block of voltage-activated calcium channels in adult rat dorsal root ganglion neurones in culture. *British Journal of Pharmacology* **121**, 1461–1467.

Dodt, E. & Zotterman, Y. (1952). The discharge of specific cold fibres at high temperatures (the paradoxical cold). *Acta Physiologica Scandinavica* **26**, 358–365.

DUBNER, R., SUMINO, R. & WOOD, W. I. (1975). A peripheral 'cold' fiber population responsive to innocuous and noxious thermal stimuli applied to monkey's face. *Journal of Neurophysiology* **38**, 1373–1389.

GEE, M. D., LYNN, B., BASILE, S., PIERAU, F. K. & COTSELL, B. (1999). The relationship between axonal spike shape and functional modality in cutaneous C-fibres in the pig and rat. *Neuroscience* **90**, 509–518.

HARRISON, S. M. & BERS, D. M. (1987). The effect of temperature and ionic strength on the apparent Ca-affinity of EGTA and the analogous Ca-chelators BAPTA and dibromo-BAPTA. *Biochimica et Biophysica Acta* **925**, 133–143.

HENSEL, H. (1981). *Thermoreception and Temperature Regulation.* Academic Press, London.

HENSEL, H. & SCHÄFER, K. (1974). Effects of calcium on warm and cold receptors. *Pflügers Archiv* **352**, 87–90.

HENSEL, H. & ZOTTERMAN, Y. (1951*a*). The effect of menthol on the thermoreceptors. *Acta Physiologica Scandinavica* **24**, 27–34.

HENSEL, H. & ZOTTERMAN, Y. (1951*b*). The response of the cold receptors to constant cooling. *Acta Physiologica Scandinavica* **22**, 96–105.

HILLE, B. (1992). *Ionic Channels of Excitable Cells.* Sinauer Associates Inc., Sunderland, Massachusetts.

IRIUCHIJIMA, J. & ZOTTERMAN, Y. (1960). The specificity of afferent cutaneous C fibres in mammals. *Acta Physiologica Scandinavica* **49**, 267–278.

KAPLAN, D. R. & MILLER, F. D. (2000). Neurotrophin signal transduction in the nervous system. *Current Opinion in Neurobiology* **10**, 381–391.

KENSHALO, D. R. (1970). Psychophysical studies of temperature sensitivity. *Contributions to Sensory Physiology* **4**, 19–74.

KENSHALO, D. R. & DUCLAUX, R. (1977). Response characteristics of cutaneous cold receptors in the monkey. *Journal of Neurophysiology* **40**, 319–332.

KOPLAS, P. A., ROSENBERG, R. L. & OXFORD, G. S. (1997). The role of calcium in the desensitization of capsaicin responses in rat dorsal root ganglion neurons. *Journal of Neuroscience* **17**, 3525–3537.

LATTANZIO, F. A. (1990). The effects of pH and temperature on fluorescent calcium indicators as determined with Chelex-100 and EDTA buffer systems. *Biochemical and Biophysical Research Communications* **171**, 102–108.

LEEM, J. W., WILLIS, W. D. & CHUNG, J. M. (1993*a*). Cutaneous sensory receptors in the rat foot. *Journal of Neurophysiology* **69**, 1684–1699.

LEEM, J. W., WILLIS, W. D., WELLER, S. C. & CHUNG, J. M. (1993*b*). Differential activation and classification of cutaneous afferents in the rat. *Journal of Neurophysiology* **70**, 2411–2424.

LINDSAY, R. M., EVISON, C. J. & WINTER, J. (1991). Culture of adult mammalian peripheral neurones. In *Cellular Neurobiology: A Practical Approach*, ed. CHAD, J. & WHEAL, H. V., pp. 3–17. IRL Press/Oxford University Press, Oxford.

LIU, L. & SIMON, S. A. (1997). Capsazepine, a vanilloid receptor antagonist, inhibits nicotinic acetylcholine receptors in rat trigeminal ganglia. *Neuroscience Letters* **228**, 29–32.

LONG, R. R. (1977). Sensitivity of cutaneous cold fibers to noxious heat: paradoxical cold discharge. *Journal of Neurophysiology* **40**, 489–502.

MCKEMY, D. D., NEUHAUSSER, W. M. & JULIUS, D. (2002). Identification of a cold receptor reveals a general role for TRP channels in thermosensation. *Nature* **416**, 52–58.

MAINGRET, F., LAURITZEN, I., PATEL, A. J., HEURTEAUX, C., REYES, R., LESAGE, F., LAZDUNSKI, M. & HONORÉ, E. (2000). TREK-1 is a heat-activated background K$^+$ channel. *EMBO Journal* **19**, 2483–2491.

MORI, Y., INOUE, R., ISHII, M., HARA, Y. & IMOTO, K. (2001). Dissecting receptor-mediated Ca^{2+} influx pathways: TRP channels and their native counterparts. *Japanese Journal of Pharmacology* **87**, 245–252.

OKAZAWA, M., TAKAO, K., HORI, A., SHIRAKI, T., MATSUMURA, K. & KOBAYASHI, S. (2002). Ionic basis of cold receptors acting as thermostats. *Journal of Neuroscience* **22**, 3994–4001.

OKAZAWA, M., TERAUCHI, T., SHIRAKI, T., MATSUMURA, K. & KOBAYASHI, S. (2000). *l*-menthol-induced [Ca^{2+}]$_i$ increase and impulses in cultured sensory neurons. *Neuroreport* **11**, 2151–2155.

OLIVER, A. E., BAKER, G. A., FUGATE, R. D., TABLIN, F. & CROWE, J. H. (2000). Effects of temperature on calcium-sensitive fluorescent probes. *Biophysical Journal* **78**, 2116–2126.

PATAPOUTIAN, A. & REICHARDT, L. F. (2001). Trk receptors: mediators of neurotrophin action. *Current Opinion in Neurobiology* **11**, 272–280.

PEIER, A. M., MOQRICH, A., HERGARDEN, A. C., REEVE, A. J., ANDERSSON, D. A., STORY, G. M., EARLEY, T. J., DRAGONI, I., MCINTYRE, P., BEVAN, S. & PATAPOUTIAN, A. (2002). A TRP channel that senses cold stimuli and menthol. *Cell* **108**, 705–715.

PETRUSKA, J. C., COOPER, B. Y., GU, J. G., RAU, K. K., & JOHNSON, R. D. (2000*a*). Distribution of P2X1, P2X2, and P2X3 receptor subunits in rat primary afferents: relation to population markers and specific cell types. *Journal of Chemical Neuroanatomy* **20**, 141–162.

PETRUSKA, J. C., NAPAPORN, J., JOHNSON, R. D., GU, J. G. & COOPER, B. Y. (2000*b*). Subclassified acutely dissociated cells of rat DRG: histochemistry and patterns of capsaicin-, proton-, and ATP-activated currents. *Journal of Neurophysiology* **84**, 2365–2379.

PIERAU, F., TORREY, P. & CARPENTER, D. (1974). Mammalian cold receptor afferents: role of an electrogenic sodium pump in sensory transduction. *Brain Research* **73**, 156–160.

PIERAU, F. K., TORREY, P. & CARPENTER, D. (1975). Effect of ouabain and potassium-free solution on mammalian thermosensitive afferents *in vitro*. *Pflügers Archiv* **359**, 349–356.

RAE, J., COOPER, K., GATES, P. & WATSKY, M. (1991). Low access resistance perforated patch recordings using amphotericin B. *Journal of Neuroscience Methods* **37**, 15–26.

REID, G., AMUZESCU, B., ZECH, E. & FLONTA, M.-L. (2001). A system for applying rapid warming or cooling stimuli to cells during patch clamp recording or ion imaging. *Journal of Neuroscience Methods* **111**, 1–8.

REID, G. & FLONTA, M.-L. (2001*a*). Cold current in thermoreceptive neurons. *Nature* **413**, 480.

REID, G. & FLONTA, M.-L. (2001*b*). Cold transduction by inhibition of a background potassium conductance in rat primary sensory neurones. *Neuroscience Letters* **297**, 171–174.

REID, G. & FLONTA, M.-L. (2002). Ion channels activated by cold and menthol in cultured rat dorsal root ganglion neurones. *Neuroscience Letters* **324**, 164–168.

RUPPERSBERG, J. P. & RUDEL, R. (1983). A simple method for controlling the fluid level in a small experimental chamber during slow and rapid fluid exchange. *Pflügers Archiv* **397**, 158–159.

SCHÄFER, K. (1987). A quantitative study of the dependence of feline cold receptor activity on the calcium concentration. *Pflügers Archiv* **409**, 208–213.

SCHÄFER, K. & BRAUN, H. (1990). Modulation of periodic cold receptor activity by ouabain. *Pflügers Archiv* **417**, 91–99.

SCHÄFER, K., BRAUN, H. A. & HENSEL, H. (1982). Static and dynamic activity of cold receptors at various calcium levels. *Journal of Neurophysiology* **47**, 1017–1028.

SCHÄFER, K., BRAUN, H. A. & HENSEL, H. (1984). Temperature transduction in the skin. In *Thermal Physiology*, ed. Hales, J. R. S., pp. 1–11. Raven Press, New York.

Schäfer, K., Braun, H. & Isenberg, C. (1986). Effect of menthol on cold receptor activity. Analysis of receptor processes. *Journal of General Physiology* **88**, 757–776.

Shu, X. & Mendell, L. M. (2001). Acute sensitization by NGF of the response of small- diameter sensory neurons to capsaicin. *Journal of Neurophysiology* **86**, 2931–2938.

Shuttleworth, T. J. & Thompson, J. L. (1991). Effect of temperature on receptor-activated changes in $[Ca^{2+}]_i$ and their determination using fluorescent probes. *Journal of Biological Chemistry* **266**, 1410–1414.

Spray, D. C. (1974). Metabolic dependence of frog cold receptor sensitivity. *Brain Research* **72**, 354–359.

Suto, K. & Gotoh, H. (1999). Calcium signaling in cold cells studied in cultured dorsal root ganglion neurons. *Neuroscience* **92**, 1131–1135.

Takahashi, A., Camacho, P., Lechleiter, J. D. & Herman, B. (1999). Measurement of intracellular calcium. *Physiological Reviews* **79**, 1089–1125.

Thut, P. D. & Gold, M. S. (2001). Cold transduction in rat trigeminal ganglion neurons (TGN) *in vitro*. *Society for Neuroscience Abstracts* **27,** program no. 707.1.

Viana, F., De La Peña, E. & Belmonte, C. (2002). Specificity of cold thermotransduction is determined by differential ionic channel expression. *Nature Neuroscience* **5**, 254–260.

Winston, J., Toma, H., Shenoy, M. & Pasricha, P. J. (2001). Nerve growth factor regulates VR-1 mRNA levels in cultures of adult dorsal root ganglion neurons. *Pain* **89**, 181–186.

Supplementary material

The online version of this paper can be found at:

http://www.jphysiol.org/cgi/content/full/545/2/595

and contains further detail about the groups and numbers of neurones included in this study.